Chapter 8
Pre-Instrumental Earthquakes Along the Dead Sea Rift

Amotz Agnon

Abstract The Dead Sea rift offers a wealth of information about pre-instrumental earthquakes. The types of potential archives include historic seismicity, archaeological sites, disturbed beds in lake deposits, rockfalls within caves as well as on free slopes, and displaced marine terraces. The rich historical archive is useful as a key for deciphering the geological archives.

Of the geological archives developed for the Dead Sea rift, lake sections stand out due to the long periods covered with high resolution. Lake deposits contain long and potentially continuous archives of the environment, and of earthquakes in particular. The Holocene drop in Dead Sea level, accentuated with a fast anthropogenic drop, have triggered incision and outcrop formation, permitting access and direct investigation of archives. The ongoing analysis of cores from lake drill-holes will augment the continuity of the archive.

The historical information spans periods that exceed the seismic cycle of individual fault segments. One of the provoking results of the comparisons of historical versus geological archives of earthquake activity is the significant difference in the apparent length of the earthquake cycle, where prehistorical data indicates long quiescence periods. This suggests that even the long historical record of the Levant does not encompass the full earthquake cycle along the entire Dead Sea fault. This result underscores the significance of paleoseismic research for the understanding of earthquake-fault mechanics and for hazard assessment.

Keywords Paleo-earthquakes • Earthquake clustering • Historic earthquakes • Dead Sea earthquakes

A. Agnon (✉)
The Fredy and Nadine Herrmann Institute of Earth Sciences, The Hebrew University of Jerusalem, Edmond J. Safra campus, Givat Ram, Jerusalem 91904, Israel
e-mail: amotz@huji.ac.il

Z. Garfunkel et al. (eds.), *Dead Sea Transform Fault System: Reviews*,
Modern Approaches in Solid Earth Sciences 6, DOI 10.1007/978-94-017-8872-4_8,
© Springer Science+Business Media Dordrecht 2014

8.1 Introduction

The study of pre-instrumental earthquakes has made considerable progress in the world during the last 40 years since the introduction of geological observations to a subject previously dominated by historic research. Paleoseismology has opened a new dimension in the study of recurrence and magnitudes of past earthquakes (Sieh 1978; Swan et al. 1980; Yeats et al. 1997; McCalpin 2009). Paleo-earthquake research is essential for the study of any fault system for which the loading-unloading cycle is longer than the period covered by history.

The historical archive for the Dead Sea rift (DSR) is extensive over the last three millennia and, at times, includes complementary sources from coexisting cultures (Guidoboni et al. 1994; Ambraseys et al. 1994; Guidoboni and Comastri 2005; Karcz 2004; Sbeinati et al. 2005; Ambraseys 2005a, b, 2009).

The value of pre-instrumental seismicity has been underscored by several authors, and several articles have reviewed preinstrumental earthquakes in the Levant (see Garfunkel 2011, for a recent review). Ambraseys (1971) has detected a pattern of interaction in catalogues of historic earthquakes along the two conjugate faults that bound the Anatolian block (NAF and EAF in Fig. 8.1). Karcz et al. (1977) have used archaeological evidence to test historical catalogues, and found a different distribution of damage, where the former exhibit higher concentration along the rift. Garfunkel et al. (1981) have used historic earthquakes to identify a spatio-temporal

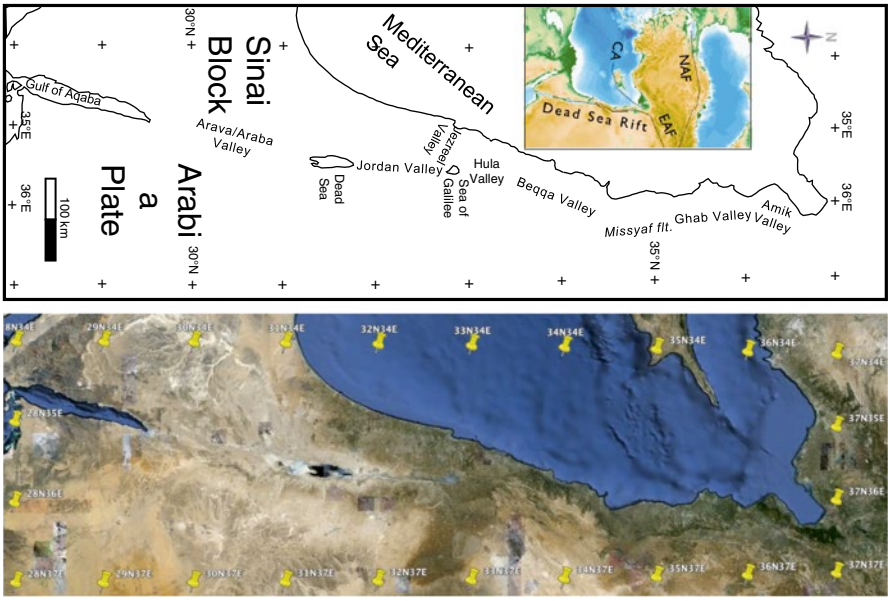

Fig. 8.1 Basins along the Dead Sea rift. *Inset* shows the adjacent plate boundaries: *EAF* East Anatolian fault, *CA* Cypriot arc, *NAF* North Anatolian fault (Generated by http://woodshole.er.usgs.gov/mapit/). Lower panel - from © 2012 GoogleEarth

pattern of seismic gaps. Stiros (2001) has used historical accounts, archaeological excavations, and geological observations for identifying a cluster of activity that spanned three centuries along four plate boundaries in the Eastern Mediterranean, including the Dead Sea rift. Agnon et al. (2006) have reviewed recent research focused on lake sediments for studying historic and pre-historic earthquakes. They reaffirmed temporal earthquake clustering with a long cycle of activity, of order 10 kyear, longer than the historic period.

The present review attempts to be more comprehensive, including historical, archaeological, and geological information, and spanning historical and prehistorical times. Comparison between alternative sources is given where applicable. We start with a systematic review of the sources that include historical catalogues, excavated archaeological ruins (on- and off-fault), and geological evidence of several types: lake seismites, coastal terraces with related sediments, and rock falls (in caves and on free slopes). A discussion of the extent and the reliability of each type follows its description. A following section presents the temporal correlations between the various sources. In the spirit of the present review, an attempt is made to cover all possible correlations. Subsequently we consider the issue of completeness of the archives, critical to the assessment of recurrence patterns, which comprises the discussion section.

8.2 Sources of Information

This review focuses on earthquakes recorded by off-fault effects, including collapsed and cracked buildings (from historical accounts and archaeological excavations), disturbed sediments, and displaced coastal features. Direct evidence of surface ruptures is reviewed in a different chapter (Marco and Klinger 2014), but on occasion such information is used here for supporting the present interpretations (Ellenblum et al. 1998; Gluck 2001; Haynes et al. 2006; Akyuz et al. 2006; Ferry et al. 2011; Sbeinati et al. 2010).

8.2.1 Historic Earthquakes

During the time of the development of the paleoseismic research in the Dead Sea rift, namely the last two decades, several comprehensive catalogues have been published under a modern standard. The catalogues of Ambraseys et al. (1994) and Guidoboni et al. (1994) mark the transition to such a standard. The extent of literature on historic earthquakes of the Levant is formidable, and often catalogues are conflicting and confusing, as pointed out by Karcz (2004). Since that review, focused on Jewish sources between the second century BCE and the eighth century CE, three additional catalogues have been published (Guidoboni and Comastri 2005; Sbeinati et al. 2005; Ambraseys 2009). The present review is written from a geological

perspective by a non-historian so only recent extensive regional catalogues are used systematically. When physical evidence for earthquakes support the catalogues of Ben Menahem (1991) and Amiran et al. (1994), they are used to augment the ones mentioned above. Sbeinati et al.'s (2005) catalogue is focused on the northern Levant, whereas Ambraseys et al. (1994) focus on the Red Sea; the others include areas around the Mediterranean. Ambraseys (2006a, b) filtered the larger events for which he estimated surface wave magnitudes (Ms) from macroseismic data. Salamon (2010) and Kagan et al. (2011) compiled lists of larger and generally consensual events reported in these catalogues to have shaken the Levant, and in particular the DSR.

Figure 8.2 displays sites central to the historical discussion of earthquakes (a) and interpreted locations of historic events (b–d). Some of the events require special attention due to possible bias in the historic documents and interaction with other disciplines (e.g. Karcz 2004; Ambraseys 2005a, b). Archaeological evidence for demise has been associated with historic earthquakes even when the dating of damaged structures was poorly constrained. Thus questionable dating could be presented as infallible. This approach can potentially introduce spurious interpretations of archaeological as well as historical data.

Kagan et al. (2011) have recently compiled a list of historic events that could potentially affect the Dead Sea basin, and tested for correlations between each event and dated lake seismites. They have used an attenuation relation that describes the decay of macroseismic intensity with distance from the source in the Eastern Mediterranean and Middle East (Ambraseys and Jackson 1998):

$$M_S = -1.54 + 0.65(I_i) + 0.0029(R_i) + 2.14\log(R_i) + 0.32p, \tag{8.1}$$

where M_S is estimated surface-waves magnitude and I_i is the Medvedev-Sponheuer-Karnik intensity. $R_i = \sqrt{r_i^2 + r_0^2}$ with r_i being the mean isoseismal radius of intensity I_i, and r_0=9.7 km. Equation (8.1) was based on 488 isoseismal contours that were fit to about 9,000 intensity points originating from 123 shallow instrumental earthquakes. Ambraseys (2006a, b; 2009) studied different seismogenic zones, the DSR being one of them. He adjusted the coefficients of Eq. (8.1) to macroseismic data of 59 instrumental DSR events, and obtained:

$$M_S = -0.138 + 0.554(I_i) + 0.0033(r_i) + 1.54\log(r_i) + 0.31p, \tag{8.2}$$

where r_i (in km) in the near-field is the distance from a point with the *i* th intensity to the source or its nearest rupture. Ambraseys (2006a, b, 2009) used Eq. (8.2) to assess source location and magnitude of 80 pre-instrumental events. This allowed him to calculate frequency-size distribution and rate of moment release.

Hough and Avni (2011) used extensive data by Avni (1999) from the M6.3 1927 Jericho earthquake to calibrate the attenuation relation for the region using the schemes of Bakun and Wentworth (1997). They have augmented the calibration by "did you feel it" reports for the M5.0 2005 Lebanon earthquake (Atkinson and Wald 2007). Hough and Avni (2011) extend the attenuation relation derived by Malkawi

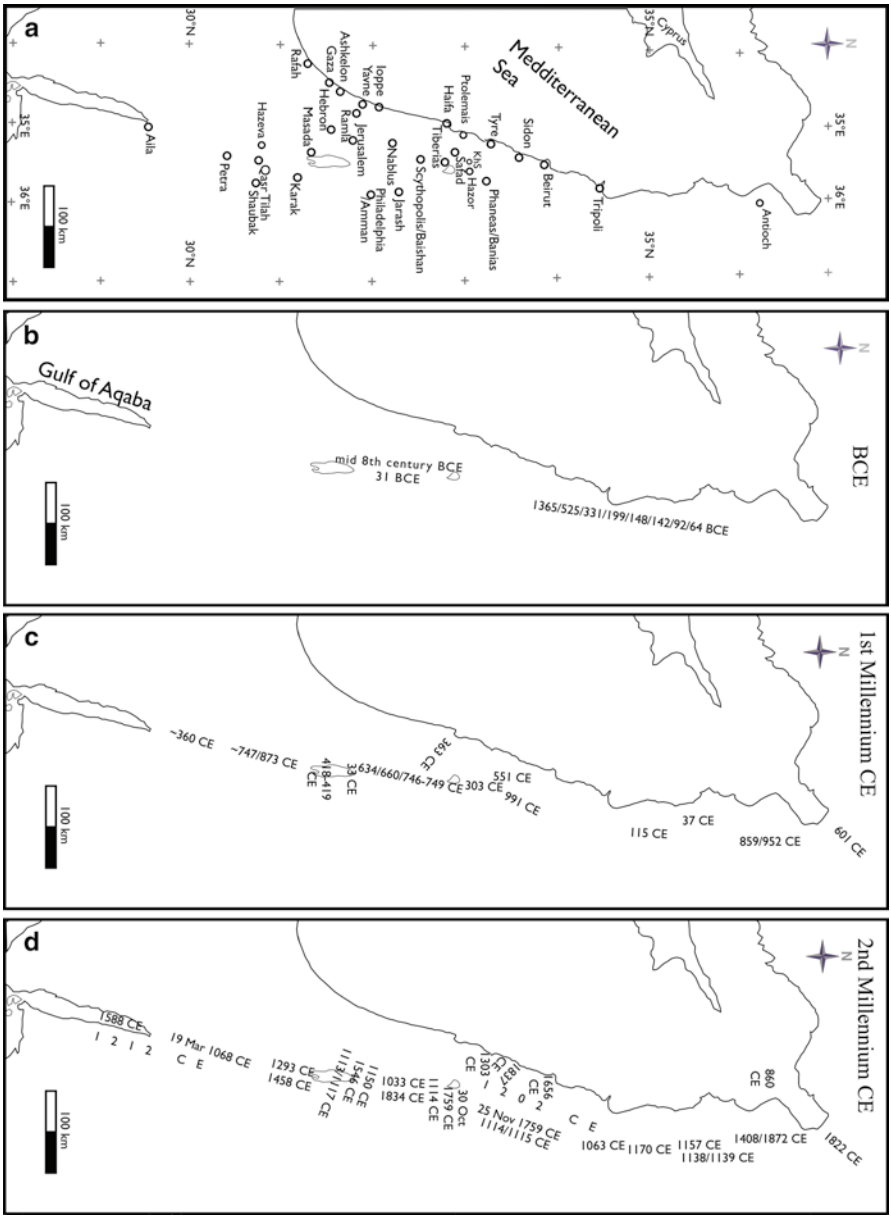

Fig. 8.2 Sites of documented historic earthquakes (**a**) and inferred source zones for BCE (**b**), 1st Millennium CE (**c**) and second Millennium CE (**d**)

and Fahmi (1996) (see review by Al-Qaryouti 2008) to include the M7.3 1995 Gulf of Aqaba event. Rearranged in the form of Eqs. (8.1 and 8.2), a preliminary calibrated attenuation relation for DSR is given by:

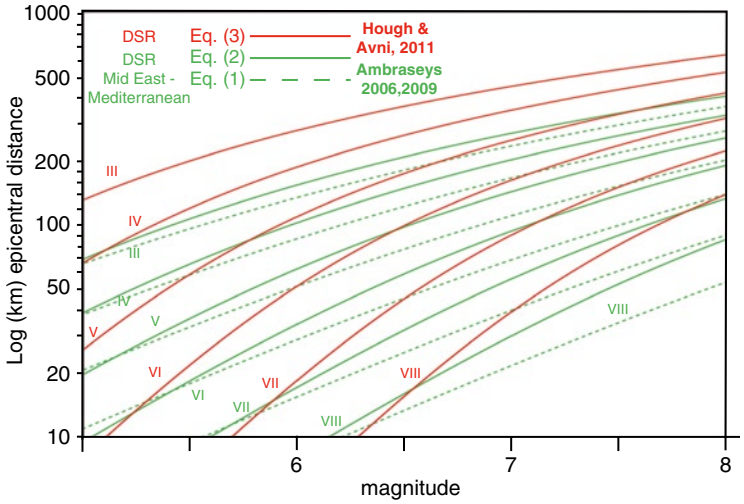

Fig. 8.3 Attenuation relations used in this and previous studies that correlate historical macroseismic data with physical evidence for earthquakes. The *curves* represent Eqs. (8.1, 8.2 and 8.3), where for Eq. (8.1) r_0 was set to null in accordance with Ambraseys (2006a, b, 2009). Setting r_0 to 9.7 km makes a minor difference

$$M = 0.388 + 0.588\left(I_i\right) + 0.00282\left(r_i\right) + 0.98\log\left(r_i\right). \tag{8.3}$$

Hough and Avni (2011) use Eq. (8.3) to assess the magnitudes of two historic earthquakes, 1170 and 1202 CE, as 6.6 and 7.6, respectively (compared with Ambraseys (2006a, b) who estimates 7.3 and 7.2 respectively).

Figure 8.3 displays Eqs. (8.1, 8.2 and 8.3) where iso-intensity lines are plotted on (log r, M) field. At small epicentral distances (<20 km) or at moderate magnitudes (<6.5) the three equations predict similar intensities (to within the scatter of the data). At large distances, Eq. (8.3) predicts intensities higher by one (low magnitude) to two (high magnitude) units. A general observation is that the curves are progressively more convex (downward) from (8.1, 8.2 and 8.3). We will return to these attenuation relations for correlation of historical seismicity and physical evidence.

8.2.2 Archaeological Evidence of Earthquakes

The DSR and its surroundings are dotted with numerous archaeological excavations that have generated reports of earthquake damage tied to particular strata and hence often associated with historic events (Fig. 8.4) (Karcz et al. 1977). As is generally the case for seismology and paleoseismology (Yeats et al. 1997; McCalpin 2009), in archaeoseismic studies the distinction between on-fault and off-fault phenomena is

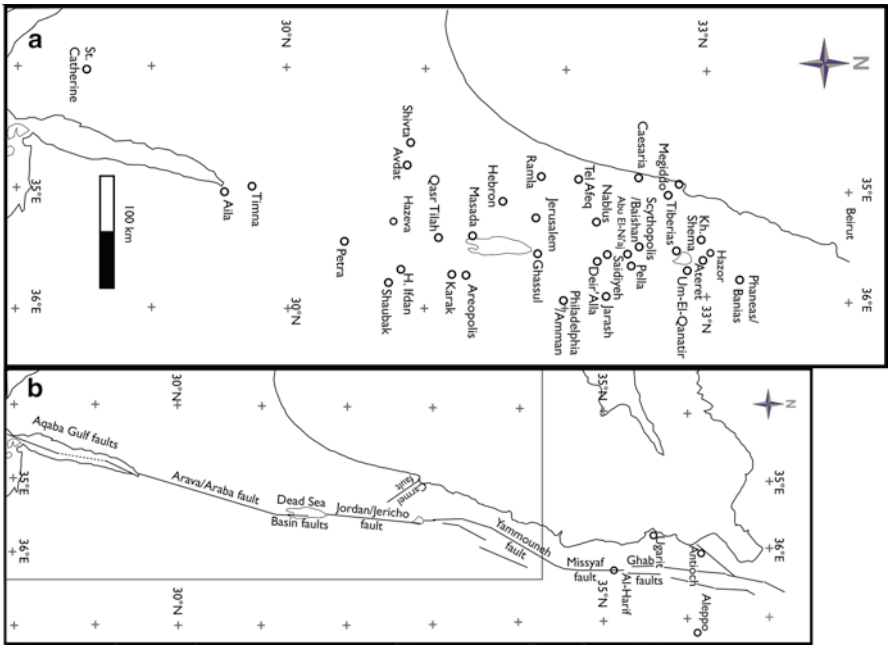

Fig. 8.4 Archaeological sites where earthquake evidence has been reported (**a**) The main fault segments forming the Dead Sea Rift are shown (**b**)

central. The DSR is unique in that it offers clear cases of on-fault archaeoseismic sites. Marco (2008) has recently reviewed archaeoseismic studies along the Dead Sea rift. In this section we present cases that are pertinent to the present discussion.

The study of earthquakes via the archaeology of ruins should benefit from close collaboration between geologists and archaeologists (and historians if the period in question is documented in chronicles). Coauthoring of papers with archaeologists increases the prospects for professional reading of the archaeology (Karcz et al. 1977; Marco et al. 1997, 2006; Ellenblum et al. 1998; Marco et al. 2003; Shaked et al. 2004; Thomas et al. 2007; Wechsler et al. 2009; Sbeinati et al. 2010; Ferry et al. 2011). The first example described below is a unique case where excavations have been systematically driven and steered in collaboration between a historian and earthquake geologists, where the on-site archaeologists made their operational decisions in order to address seismological issues.

8.2.2.1 Tel Ateret

The most striking example of an on-fault archaeoseismic study is the excavations of Tel-Ateret (Fig. 8.5). Marco et al. (1997) have documented the Crusader castle of Vadum Iacob (Tel Ateret) over which an Ottoman mosque had been constructed, respectively offset sinistrally 2.1 and 0.5 m (Fig. 8.5). Ellenblum et al. (1998) have

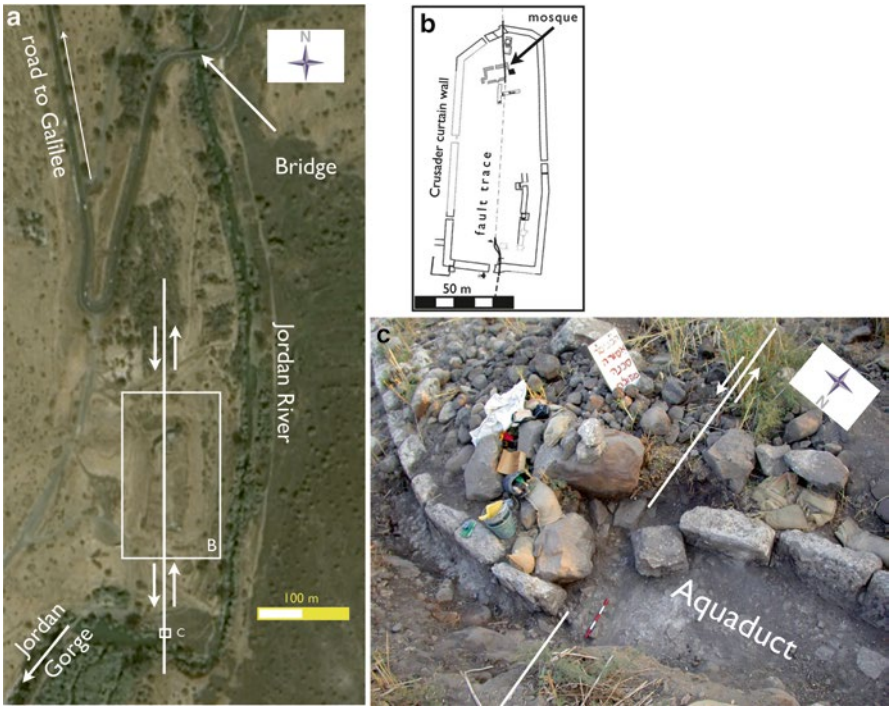

Fig. 8.5 Tel Ateret. (**a**) A satellite photo (GoogleEarth) of the Ateret – Benot Ya'aqov bridge. Vadum Iacob castle straddles the fault trace, that runs through an aqueduct system south of the castle. (**b**) The outline of Vadum Iacob Crusader castle (curtain wall) and the Ottoman mosque. (**c**) Aqueduct photo taken down and to the south-south-west. The *red*-and-*white scale* is 0.5 m aligned north to south

assigned individual earthquakes to the two offset events: 20 May 1202 CE (1.6 m) and 30 October 1759 (0.5 m). These earthquakes have been independently assigned macroseismic magnitudes of 7.2 (Ambraseys 2006b) and 6.5 (Ambraseys and Barazangi 1989). The macroseismic magnitudes are compatible with displacement-magnitude systematics (Wells and Coppersmith 1994).

The advantage of archaeology is its precision in determining the amounts slip. When combined with history, archaeology can resolve the timing of slip events as no other method can. The Crusader's curtain wall was meticulously laid, allowing a precision approaching 1 cm. The Ottoman wall allowed ~0.1 m precision. Very similar and synchronous offsets, albeit with lower precisions in amount and date, have been recorded by paleoseismic trenching of fluvial channels some 10 km south of Tel Ateret (Marco et al. 2005; Marco and Klinger 2014).

Meghraoui et al. (2003) and Sbeinati et al. (2010) reconstruct an offset aqueduct at Al-Harif, where they assign an offset of 13 m and an age of ~2 ka (Fig. 8.4b). The challenge with deciphering offset from aqueducts is often the lack of control on initial, pre-deformation structure. In addition, archaeological dating of damage to an

aqueduct is not as precise as dating of living quarters, where one may find a wealth of well dated artifacts, and floors that demonstrate a stratigraphic context, constraining the age of the vertical features. Not only the destruction of aqueducts is difficult to date, their construction date is typically vague for similar reasons. We have excavated an aqueduct at the site of Tel Ateret and, ironically, it is dated based on its left-lateral offset of 2 m, similar to the offset of the nearby Crusader's castle (Fig. 8.5c).

The dating of the earthquakes associated with the offset of Vadum Iacob are exceptionally well constrained by history, documented both by Crusaders and Muslims. The castle was erected during 11 months and, before completion, conquered and demolished by Saladin in late August, 1179 CE (Ellenblum 2007). The floor at the time of construction and conquest stands out due to its conspicuous lime color and richness with metallic weapons and construction tools. In the subsequent 22.5 years, thin (several-cm scale) soil accumulated on the rubble to be ruptured during the earthquake of 20 May 1202 CE. A meter (or more) of soil has accumulated during the last eight centuries. A fraction of this soil layer (30 % or more) was ruptured during the 30 Oct 1759 M ~ 6.5 event.

8.2.2.2 Qasr Tilah

An additional case where the DSR or its branches offset archaeological structures have been documented, where the archaeological context jointly with radiocarbon dates allow particular earthquakes to be suggested. A water reservoir and an associated aqueduct in Qasr Tilah, south of the Dead Sea (Fig. 8.4), are offset by about 2 m (Klinger et al. 2000; Haynes et al. 2006). The dates of damage from the last four rupture events was correlated by Haynes et al. (2006) to the historic earthquakes of 634 or 659/660, 873, 1068, and an Ottoman Period event. The assignment to a seventh century CE earthquake was based on dates of construction and repair during the occupation of the site, that has seemed to be abandoned during later centuries. Haynes et al. (2006) have assigned a historic earthquake from 873 CE to the second rupture at a paleoseismic trench. The epicenter of 873 CE earthquake was placed by Ambraseys et al. (1994) well in the Arabian Plate, yet Haynes et al. (2006) suggest that due to sparse population the catalogue is biased. Haynes et al. (2006) disregard the possibility that one of the mid eighth century earthquakes was candidate. Bikai (2002) attributes collapse of the Blue Chapel to the mid-eighth century AD earthquake. Eklund (2008) infers widespread destruction by a mid-eighth century earthquake, and this may suggest rupture during this time south of the Dead Sea.

The third rupture in the trench, being the penultimate event, crosses a layer of seventh–tenth century CE dated by Haynes et al. (2006), who suggest the earthquake of 18 March 1068. Haynes et al. (2006) select the earthquake of 1546 as the best candidate for the most recent event to rupture Qasr Tilah, since the layer cut during this rupture is dated to the Ottoman period (1515–1918 CE). The earthquake of 1546 was played down by Ambraseys and Karcz (1992) as one that affected only Jerusalem, hence being exaggerated. An alternative is the earthquake of 1834 with reported damage from Karak to Caesarea (Fig. 8.2) and asphalt emissions in the

Dead Sea (Amiran et al. 1994; Ambraseys 2009). Garfunkel et al. (1981) interpreted this event as a rupture in the Dead Sea and northern Arava, based on the then available catalogues. Ben-Menahem (1991) placed the 1834 epicenter at the southern dead sea, noting toppling of structures east of the Dead Sea. More data is needed for ruling between the historic earthquakes of 1546 and 1834 as the ultimate event in Qasr Tilah.

8.2.2.3 Fallen and Cracked Off-fault Structures

Severe ground shaking having caused structural destruction can be recorded and subsequently unearthed in archaeological sites. Marco (2008) has surveyed some cases of fallen and cracked masonry structures to exemplify useful diagnostics for earthquake related damage. Additional cases, some mentioned by Russell (1980) include Petra, Sephourias, Bet Shearim, and Scythopolis for the 363 earthquake, and several others. Distinct features that testify for earthquake damage include lack of evidence for alternative causes of damage, and special features such as human skeletons in positions indicating attempts for self-protection (Nur 2008).

Archaeology often extends the seismic record beyond the historic period. An ongoing collaboration between archaeologists and geologists enabled the interpretation of destruction layers and masonry damage in Megiddo (Fig. 8.4), perpetually reconstructed for twenty-six centuries (e.g. Porat et al. 2012). This site offers unique data on the Carmel fault branch of the Dead Sea rift. Marco et al. (2006) have documented 18 instances of damage, of which 16 may have resulted from seismic shaking. They denote ten of the cases as "probably catastrophic", of which seven indicate shaking (four of them horizontal). In a single case, a liquified sand bed is taken as clear evidence of catastrophic shaking. Altogether, the damage seems to had happened in six events, where at least two of them had been caused by earthquakes: shortly before 5 ka and between 2.8 and 2.9 ka. Another likely event preceded the latter by about a century. Evidence for additional events lacks confidence in source of damage or dating, or both. The likely source of the earthquake damage is rupture on the Carmel fault that runs apparently underneath the site (Fig. 8.4), yet the Jordan fault, less than 40 km away, is a viable candidate.

Russell (1980) and Hammond (1980) have based their arguments for a large 363 earthquake, damaging the entire southern sector of the continental DSR, on the collapse of the Temple of the Winged Lions in Petra and destruction at the Main Theatre (Fig. 8.6a). This dramatic finding matched well with the concept of a drastic decline of Petra during the fourth–fifth century CE up to a complete abandonment following destruction by a mid sixth century earthquake, namely 551 CE. The excavations of 1991–1993, that have casted doubt on damage by the 551 CE event. These excavations have demonstrated that the site continued to function to a final destruction during the very late eighth century or the ninth century CE (Eklund 2008). The impressive collapse of a colonnade from the Great Temple, likely due to an earthquake (Fig. 8.6b) is yet to be dated.

Fig. 8.6 colonnades (**a**) Temple of Winged Lions; (**b**) Great Temple; (**c**) Hippos SE church; (**d**) Hippos NW church

Some archaeological sites show damage in more than a single layer. Tsafrir and Foerster (1997) documented impressive damage from a 363 CE earthquake to Scythopolis. Earthquake damage from 363 CE has been cited by many authors for many sites (e.g. Russell 1980). Scythopolis was hit again early-to-mid seventh century CE before seismogenic demolition (under the Arab name Baishan) during the mid-eighth century CE. Tsafrir and Foerster (1997) used numismatic evidence to date the latter event as 749 CE. Karcz (2004) pointed out that this find does not rule out an earlier event (747 CE) while Ambraseys (2009) argued that the case is not closed without ruling out later events (757 or 768–775 CE). All these discussions underscore the precision available in historical documents buttressed by archaeological evidence which allow accuracy not attainable in purely geochronological studies. However, geological evidence can help when the resolution is sufficient, as discussed below in the "Correlation" section.

The attribution of damage in ruins to earthquakes in general and to particular historical temblors is often challenged. Magness (1997) has argued against the assignments of a pair of earthquakes, 306 CE and 419 CE, to damage in Khirbet Shema' (Fig. 8.2a) (Meyers et al. 1976). The argument is based on a lack of positive evidence of earthquake destruction at 306 CE; Meyers et al. (1976) merely present precise numismatic evidence for prominent occupation between 306 and 341 CE, interpreting it as a building phase following a putative earthquake. Magness (1997) have accepted the evidence for earthquake destruction of the top layer, but assigns it to the mid-eighth century CE, long after abandonment of the site. This case demonstrates the sensitivity of earthquake chronologies derived from archaeology to the assumptions at the basis of the interpretation.

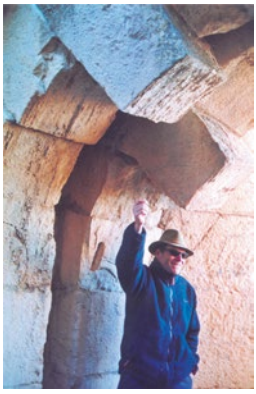

Fig. 8.7 Qal'at Subayba keystone

Several authors have commented on the circular reasoning and feed back between archaeological, historical, and geological interpretations, giving rise to false identifications (Karcz and Kafri 1978; Karcz 2004; Ambraseys 2005b, 2009; Rucker and Niemi 2010). The case of Qal'at Subayba is a useful example for the pitfalls (Figs. 8.3 and 8.7). Nur (2008) have attributed the damage in Qal'at Al-Subayba ("Qal'at Namrud") to the 1202 CE earthquake, whilst the damaged building was only erected later around 1230 and buttressed only towards 1260 (Ellenblum 1989). This precise dating is based on massive inscriptions in the site (Amitai 1989). The damage, erroneously attributed by Nur (2008) to the 1202 CE earthquake, is likely dated to the earthquake of 30 October 1759 CE (Hartal 2001).

A comprehensive and critical review of historic earthquake catalogues versus archaeological and geological evidence from DSR, a long overdue foundation for earthquake research and hazard assessment, is beyond the scope of this paper. Yet the Correlation section below discusses some promising research opportunities.

8.2.3 Lake Seismites

Seilacher (1969) pioneered the systematic identification of beds deformed at the water-sediment interface during earthquakes. He has coined the genetic term "seismite" for sedimentary rocks displaying structures that can be interpreted to result from earthquake shaking. Several types of textures in lacustrine facies have been since recognized:

1. Liquefied and fluidized beds: structures indicating folding and intrusion of coarse grain layers (Sims 1973, 1975).
2. Intraclast breccias (mix layers): beds comprising of clasts derived from the local pre-shaking sediment (Marco et al. 1996; Agnon et al. 2006).
3. Homogenites: Homogeneous massive intervals in the otherwise layered to laminated section; the composition within the homogenite is identical to a homog-

enous mixture of the compositions of the different layers or laminae (Chapron et al. 1999, following Cita et al. 1984).
4. Turbidites and silt layers: graded bedding, typically a thin bed of coarser material within fines (Siegenthaler et al. 1987, and Doig 1990, following Heezen and Ewing 1952).

Sims (1973) has underscored the potential in the study of earthquakes in active continental zones from liquefaction structures in lacustrine beds. He subsequently analyzed late Quaternary sections and inferred recurrence intervals (Sims 1975). Hempton and Dewey (1983) described a sequence of five seismites in the East Anatolia fault (EAF, Fig. 8.1), and interpreted one to reflect higher shaking intensity. With the absence of age data they used spacing for conjecturing a non regular recurrence pattern. Siegenthaler et al. (1987) have attributed a homogenite to slumping during seiche triggered by a historic earthquake in Lake Lucerne, Switzerland. They identified such homogenites in cores and seismic reflection profiles and opened the way to reconstruction of recurrence intervals and patterns. Doig (1990, 1991) had observed discoloration in small lakes at the epicentral zone of an instrumentally recorded earthquake in Canada. He inferred that graded silty layers penetrated in short cores represent earthquake induced slumping in the catchment (Doig 1998). Correlation with historic events based on constant sedimentation rate and extrapolation to prehistorical times revealed variable recurrence rates.

Marine paleoseismology has developed in parallel to lacustrine paleoseismology (Kastens 1984; Adams 1990; Roep and Everts 1991; Cita et al. 1996; Moretti et al. 1999; McHugh et al. 2006; Monecke et al. 2006; Moretti and Sabato 2007), where the distinction between seismites and other structures reflecting high mechanical energy has remained a challenge (Cita et al. 1984). In a recent issue devoted to soft sediment deformation triggered by earthquakes (Owen et al. 2011, and references therein), Gibert et al. (2011) have cast doubts on the inference of earthquake histories from one of the most common sedimentary structures used to infer earthquake shaking, namely load structures: multiple superimposed liquified layers may result from a single shaking event. Therefore, seismites that evidently formed at the water sediment interface are more useful for determining the timing of individual events and recurrence patterns.

While lacustrine paleoseismology has flourished elsewhere (e.g. Davenport and Ringrose 1987; Jones and Omoto 2000; Waldmann et al. 2011), certain properties of the sediments in the Dead Sea and its ancestral lakes (Lake Lisan in particular) have enabled unique contributions to the discipline.

8.2.3.1 Prehistoric Dead Sea Seismites

Laminated lacustrine sediments, common around the Dead-Sea Basin (Fig. 8.8), provide a recorder of high energy events at the lake bottom (Manspeizer 1985). The last global glacial cycle and the ensuing rise of lake level have deposited laminar, perhaps varved, sedimentary sections dominated by alternation of detrital and pure aragonite laminae (Begin et al. 1974; Katz et al. 1977; Barkan et al. 2001). Aragonite,

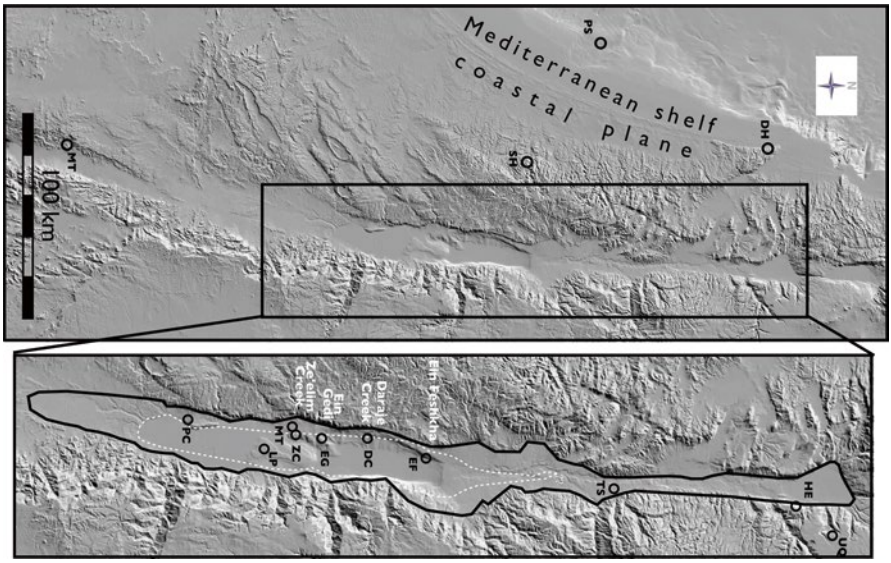

Fig. 8.8 Extent of late Pleistocene lakes and locations of paleoseismic study sites in the area. *White curve* Lisan Formation, *White broken curve* Ze'elim Formation, *PC* Pratzim Creek, *LP* Lisan Peninsula, *MT* Masada Terrace, *ZC* Ze'elim Creek, *DC* Daraje Creek, *EG* Ein Gedi, *EF* Ein Feshkha, *HE* Ha'Onn Escarpment, *SH* Soreq and Hartuv Caves, *DH* Denia Cave at Haifa, *PS* Palmahim slump. The *shaded* relief map is by Hall (1996)

a polymorph of calcium carbonate, has the advantage of preserving the primary chemistry and isotopic composition (Katz et al. 1977), hence allowing radiometric dating (Haase-Schramm et al. 2004; Stein 2011). A typical facies in the Lisan Formation comprises alternations of dark detritus versus pure white aragonite, deposited during periods of a stratified lake (Katz et al. 1977). These can be explained as seasonal laminae, or varves, where the detritus was transported to the lake during flash floods and subsequent evaporation led to aragonite precipitation (Katz et al. 1977; Barkan et al. 2001).

Laminated sections are found up to levels of ~200 m below sea level (b.s.l., where during the twentieth century A.D. the level declined below 400 m b.s.l. (Bookman et al. (2004))). The late Pleistocene Lisan Formation line the valley floor on a stretch 275 km long; the Holocene Ze'elim Formation stretches about 170 km (Fig. 8.8). The Lisan Formation (Shaw 1947) has long been recognized for unique study opportunities due to lithological uniformity, high resolution stratigraphy, and well exposed beach deposits (Bowman 1971; Bartov et al. 2002). The unit has been studied extensively in recent years (e.g. Haase-Schramm et al. 2004; Enzel et al. 2006; Ron et al. 2007; Belmaker et al. 2007; Torfstein et al. 2008; Prasad et al. 2009). The distortion and destruction of lamination in the otherwise laminated sediments of Lisan Formation has been used as an indicator for paleo-earthquakes by several authors (Pettijohn and Potter 1964; Seilacher 1984; El-Isa and Mustafa 1986; Marco and Agnon 1995; Agnon et al. 2006; Heifetz et al. 2005; Katz et al.

2009; Wetzler et al. 2010; Alsop and Marco 2011). The Ze'elim Formation (Yechieli 1993) shows similar facies, with beach ridges limited to levels lower than 370 m b.s.l., and laminar aragonite lower than 400 m (Bookman et al. (2004)). The unit exhibits seismites similar to those described in Lisan Formation (Ken-Tor et al. 2001; Migowski et al. 2004; Agnon et al. 2006; Kagan et al. 2011). The upper part of the section corresponds to historic times, enabling correlation of seismites with historic earthquakes (Ken-Tor et al. 2001; Migowski et al. 2004; Agnon et al. 2006; Kagan et al. 2011).

El-Isa and Mustafa (1986) have recognized the scientific potential of intraformational structures indicating post depositional seismic shaking (seismites). They listed three categories of processes generating structures that can be used to study paleo-earthquakes. The first category includes local faulting, cracking, and slumping. The faults are normal or horizontal, of various size and age. The second category comprises effects of liquefaction: sand boils in coarser sediments and destruction of lamination in fine grain sediments. The latter is associated with loss of cohesion and "ultimate mixing of the particles". The third category of processes was the focus of El-Isa and Mustafa's (1986) work, namely folding over décollement surfaces. Marco and Agnon (1995, 2005) used detailed stratigraphy to establish a link between faulting events and phenomena of the likes of El-Isa and Mustafa's (1986), with emphasis on their first and second categories.

The Dead Sea near-shore facies exhibits the more common types of seismites. Enzel et al. (2000) have documented 11 liquified layers in fan delta Holocene sediments of Daraje Creek (DC, Fig. 8.8). These include ball-and-pillow structures, clastic dike intrusions, convolute lamination, and micro-faults.

8.2.3.2 Seismites in Beds from the Historic Period

Several authors approached late Holocene beds exposed by recent retreat of the Dead Sea lake, attempting to correlate seismites with historic earthquakes. These correlations are discussed in a separate section below. Enzel et al. (2000) identify the ultimate rupture exposed in Daraje Creek with the M = 6.2 1927 event. Ken-Tor et al. (2001) have identified eight seismites in the fan deposits of Ze'elim Creek (ZC, Fig. 8.8). They have extracted 24 radiocarbon dates from the 7 m section that featured two unconformities representing significant hiatuses. They dated these to eighth–tenth and late thirteenth–fifteenth centuries CE, paving the way for high accuracy lake level curves (Bookman et al. (2004)). They were able to correlate all eight seismites from the section studied to historic earthquakes, although some ambiguities could not be resolved with the data. In particular, a seismite deposited around 400 CE could be interpreted as 363 or alternatively ad 419 CE (see their Figs. 8.4 and 8.3b respectively). We return to the correlation between individual seismites and particular historical events in a later section.

To circumvent the hiatuses, and to access the lacustrine laminated facies appropriate for high resolution studies, Migowski et al. (2004) have collected continuous cores from the Dead Sea shores. Three coring sites along the western shore were designed

to provide lateral coverage (Fig. 8.8): Ein Feshkha (EF), Ein Gedi (EG), and Ze'elim Creek, which allowed outcrop control with Ken-Tor et al. (2001) data. They studied a core from Ein Gedi in considerable detail. The lacustrine facies, with alternations of detritus and chemical precipitates (aragonite with, in places, halite), builds 3 m of the section of Ein Gedi core, corresponding to a historic period.

Migowski et al. (2004) had counted laminae from a 2.2 m continuously laminated section under a microscope for construction of a chronological model. The age model was constructed under the following assumptions: (i) each cycle of detritus/chemical laminae represents a year of deposition; (ii) the top of IBLs correspond to years of historic earthquakes; each calibrated radiocarbon age represents a *terminus post quem* for the deposition. They resolved breccia layers as thin as 2 mm; the thickest seismite they report is 9 cm and the average 1.4 cm. They counted 22 seismites within the otherwise laminated interval and correlated them to earthquakes between the 140 BCE and 1293 CE events.

Given the uneven distributions of earthquakes in history and of IBLs in the core, a unique age model anchored by seismite-earthquake correlation to the absolute time scale seemed plausible. The correlation was constrained by four radiocarbon dates that yielded ages 100–250 years older than the historic dates of the earthquakes. This was explained by the long time of deposition for organic matter through the dense brine formed the hypolimnion. Such a dense hypolimnion, separated from the surface water, is expected for the counted interval with its facies of interlaminated aragonite and detritus (Barkan et al. 2001).

Only two deformed layers, correlative to dates of ~90 CE and ~175 CE, could not be matched with historic events. A striking example of the high resolution of this study was given by Agnon et al. (2006) who show that the 1202 CE earthquake can be resolved from the 1212 CE earthquake.

As a test for the correlation, Migowski et al. (2004) and Agnon et al. (2006) have evaluated the local intensity of historic earthquakes in the Ein Gedi site based on the historical epicenter and magnitude, with the aid of attenuation relations (Fig. 8.3). All correlated earthquakes had high expected intensities (right-lower side of the distance-magnitude diagram), whereas earthquakes that are missing from the record were expected to have low intensity (left upper side). Some medium intensity earthquakes were identified, and some were missing for the Ein Gedi core. This test corroborates the correlation of deformed layers with earthquakes and at the same time lends support to the assumption of annual laminae cycles.

Four prominent historic events did not show in the interval where laminae were counted; these events could have been masked by successive events (1063 followed by 1068 CE), or had been duplicated in the historical catalogues due to spurious reading of multiple calendars (1032 versus 1033 CE, Ambraseys et al. 1994). Agnon et al. (2006) suggested that the earthquake of 1202 CE left a faint mark, barely resolved in the successive IBL assigned by Migowski et al. (2004) to the 1212 CE event.

Agnon et al. (2006) have revised the analysis of Ken-Tor et al. (2001) using a uniform deposition rate between unconformities. With such a model they found a unique match between each of the eight seismites and a historic event. They have accounted for the masking of event horizons by subsequent earthquakes and analyzed the resolving power of the section (see below).

Kagan et al. (2011) have studied an extended section in the more lacustrine facies of Ze'elim Creek and added seismites from sections that fill in the hiatuses in the original section. Ongoing retreat of the lake has enhanced the exposure, affording a continuous section of the last three millennia. They also collected data from an additional section at Ein Feshkha in the northernmost Dead Sea (Fig. 8.8) and analyzed the outcrop data jointly with Migowski et al.'s (2004) data from Ein Gedi core.

Altogether, Kagan et al. (2011) study over a 100 seismites, half of which in the northern (truncated) Ein Feshkha section. The relative abundance of seismites in the northern section has been attributed to preferential recording of the northern extent of the rift, perhaps by waves guided through the Jordan/Jericho fault. The comparison of the three sites allows to single out events that have affected the entire basin, generating wide spread deformation dubbed "intra-basin seismites" (IBS).

Levi et al. (2006) have studied the magneto-fabrics of clastic dikes that intrude the Lisan Formation (Marco et al. 2002). They conclude that some of the dikes, in particular those showing evidence of horizontal propagation, were injected laterally during earthquake shaking. Porat et al. (2007), based on optically stimulated luminescence (OSL) dating of dike material, infer ages of between 15 and 7 ka for injection. With the caution that the mechanism for resetting the OSL signal is not yet known, they suggest that such ages can be of use in paleoseismology.

8.2.3.3 Convolute Lamination (Intraformational Folds)

Convolute lamination – a manifestation of intraformational folding in the laminated Lisan Formation – provides a spectacular manifestation for the mechanical energy that reach the normally quiet lake bottom (Fig. 8.9). Such structures have long attracted the eye of geologists who typically associate the deformation with earthquake shaking (Pettijohn and Potter 1964). El-Isa and Mustafa (1986) were the first to systematically approach the recurrence of intra-formational folds in a partial section of the Lisan Formation ~17 m thick, east of the Lisan Peninsula (Fig. 8.8). They have documented folded beds with amplitudes between 1 and 15 cm. They have assumed a relation between the amplitude of the fold and ground acceleration, and estimated respective magnitudes. The frequency-size relation derived should be regarded with care for three reasons: (1) without knowledge of the epicentral distance the magnitude estimates are minimal; (2) disregard for breccia layers may trim the strongest earthquakes from the archive; (3) the frequency of recurrence is a lower bound, as multiple events may be erroneously amalgamated (Alsop and Marco 2011). An additional source of uncertainty arises from the possibility that folding occurs at finite depth in the sediment (Gibert et al. 2011).

Heifetz et al. (2005) have noted the geometrical similarity between the convolute beds and deformation structures that develop between fluid layers. They differentiated between symmetric folds and asymmetric billow-like structures, and conjectured that the billows are precursors to a state of total turbulence, represented by breccia layers. This suggested a mechanism for the formation of folds: Kelvin Helmholtz instability (KHI) caused by vorticity transfer into a pair of layers of contrasting density (and possibly viscosity) sliding horizontally at different speeds in response

Fig. 8.9 Intraformational folds in Lisan Formation, Peratzim Creek

to a seismic shock. Such layering is bound to form in compacting muds due to fluid expulsion, hindered settling, and formation of sedimentation fronts (Thacker and Lavelle 1977).

Heifetz et al. (2005) have linearized the KHI problem and inferred a dependence of inception of billows on driving wave and sediment properties. The higher peak horizontal acceleration, the shorter the time required for fold growth; the longer the period of the driving wave, the longer the time available for fold growth; the thinner the bed undergoing folding, the smaller the acceleration required for onset of folding instability. The density difference has two contradicting effects, ultimately resulting in an inverse proportion with the threshold for billowing. Assuming small (<10 %) density contrasts (merely due to progressive dewatering) and estimating the viscosity from the seismic wave attenuation, the threshold for any folding of a layer 0.1–1 m thick under a driving frequency of 1Hz is 0.2–0.7 g (where $g \sim 10$ m/s^2). Such conditions are possible near the epicenter of a M6.2 earthquake in the Dead Sea (Oth et al. 2007). Under bottom gradients the critical acceleration is smaller.

Wetzler et al. (2010) have corroborated the KHI approach by noting a scaling in the power spectrum of the folds which is identical to that observed in other KHI systems. They have furthered the link between horizontal peak ground acceleration and the onset of folding. The KHI approach is a promising avenue for further research, and laboratory experiments on mud will be very useful for testing the application.

Two aspects of mud, a two-phase fluid, are very different from experimentally tested single phase fluids that can develop turbulence in layers via KHI. The first aspect is that mud can develop localized states that do not propagate. Lioubashevski et al. (1999) have shown that thin mud suspensions subject to vertical shaking develop localized sub-harmonic states (oscillons) known previously only in dry granular media. A more essential aspect is the expulsion of the suspending fluid (brine in the case of Dead Sea – Lisan sediments) from the grains which fossilizes the folding. This is the process that enables us to access the geometry of these dynamic states long after stabilization.

8.2.3.4 IBLs ("Mixed Layers")

Seilacher's (1969) type example for a seismite comprised sequences of three sub-units from bottom: block faulted, rubble, and liquefied. The contacts between sub-units are gradual and so is the bottom of the sequence, in contrast to the top contact that is sharp. These features are replicated in the Dead Sea seismites identified by Marco and Agnon (1995, 2005). Owing to the seasonal lamination, the Dead Sea lacustrine seismites stand out in outcrop and drill holes, allowing calibration with historic earthquakes (Ken-Tor et al. 2001; Migowski et al. 2004; Kagan et al. 2011) and offering a unique insight into the long term seismic behavior of an active plate boundary (Marco et al. 1996; Agnon et al. 2006).

Agnon et al. (2006) renamed the "mix layers" of Marco and Agnon (1995) to "intraclast breccia layers" (IBLs), a descriptive rather than a genetic term. In the typical laminated facies of the lacustrine Dead Sea Quaternary sections, these breccias form conspicuous massive intervals, where in places fragments of laminae float in a fine grain matrix (Fig. 8.10). The top contact is sharp where a single laminae can be traced overlying the breccia layer for the entire extent of outcrops (tens of meters and possibly more). By contrast, the bottom contact is gradual, in places involved with intraformational folding (Fig. 8.10). The research focus on IBLs in the late Quaternary Dead Sea initiated due to their relations with intraformational faults (Fig. 8.11). Marco and Agnon (1995) have noticed the stratigraphic relations indicating that IBLs form simultaneously with small scale faulting and formation of micro topography (scale 0.1–1 m) on the lake bed. Marco and Agnon (2005) have documented these temporal relations in detail, and Fig. 8.11 represents visually one of their examples. Striking correlation between columnar sections on faulted blocks is limited to intervals in the hanging wall (h). Three intervals are not correlated and signify events of fast subsidence of the hanging wall followed by sedimentation that fills the tectonic micro-bathymetry. Of six IBLs in a 9 m section (7 m on the footwall), three are followed directly by the three differential subsidence events. Marco and Agnon (1995, 2005) have interpreted these relations as evidence for a causative relation between faulting and IBL. Such cases of clear thickening of IBL in the hanging wall, and slumping down the fault plane, are common near Masada and in a number of additional sites. These indicate that the resuspended material settled right after local faulting, so local faulting might have driven local resuspension.

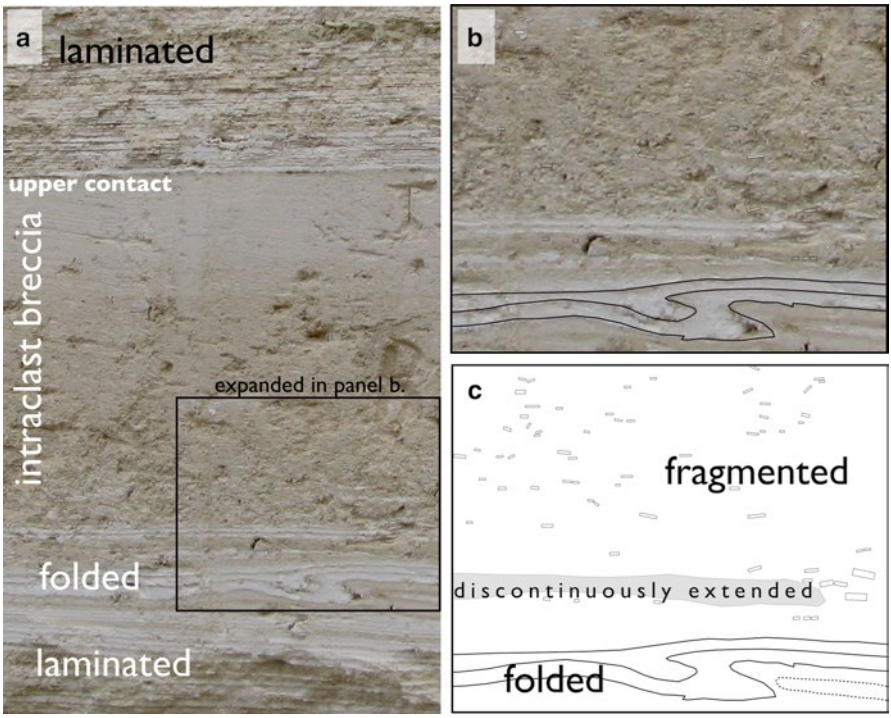

Fig. 8.10 A photograph of a sequence containing an intraclast breccia layer (**a**). (**b**) shows detail of lower contact with upward transition from folded to fragmented structures as traced in (**c**). Masada Terrace

Alternatively, faulting on a different but not too distant fault caused re-suspension and was followed by an aftershock that was related to the local fault that cause the bathymetry. In the more common setting as featured in Fig. 8.11, IBLs do not exhibit significant difference between adjacent fault blocks, so the sediment of the IBL had resuspended and resettled due to somewhat remote faulting.

The mechanism of formation of the IBLs is not yet clear, but a tentative explanation was offered by Heifetz et al. (2005) together with the mechanism for formation of convolute lamination discussed above. According to this suggestion, the transition from folding to brecciation corresponds to the transition from billows to turbulence. Such a transition is the extreme case of Kelvin-Helmholtz instability, where the drive (seismic waves) overcomes the damping due to gravity and viscosity (see Section "Intraformational folds" above).

We note the fundamental difference between KHI and Rayleigh-Taylor instability that more commonly cause seismites (e.g. Hempton and Dewey 1983): the latter depends on a gravitational drive. In Rayleigh-Taylor instability an inverse density gradient (denser on top) is rectified where the role of shaking is to overcome static friction and initiate the flow. In the case of the intraclast breccias of Lisan Formation the density gradient is normal due to compaction, and it acts to attenuate the instability. So seismic energy is required during the development of the instability, cascading

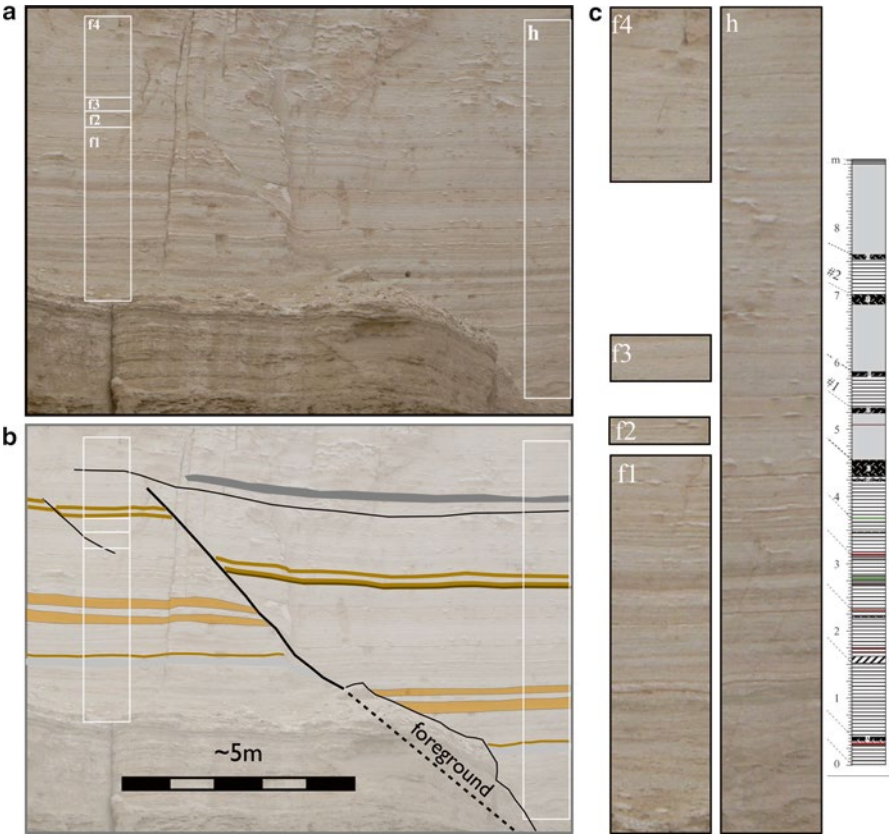

Fig. 8.11 An intraformational fault, Lisan Formation, Masada terrace. (**a**) A photograph with demarcations of selected sections expanded in panel c. (**b**) A line tracing of panel a. (**c**) Selected sections taken respectively on the foot wall (*1* and *2*) and the hanging wall (*3*). Sections are laid out to emphasize the remarkable visual correlations between the faulted blocks at the bottom and top, where the middle section of 3 is missing between 1 and 2. For lithological and attempted temporal correlation, see Marco and Agnon (2005)

into smaller scales down to the laminar scale required for complete brecciation (and to the grain scale for forming homogenites). Some gravitational energy may become available during instability because sliding on a slope is involved. The relative role of gravitational and seismic energy depends on the initial slope. The initial slope can be constrained from measurements of lateral variations in thickness of deformed units.

8.2.4 Coastal Marine Environment

DSR is one of a few transform boundaries tearing continental crust and allowing seawater to inundate some of the basins. The connection with the sea provides a datum – the global sea level, and as the case is for the DSR, coral and vermetid reef

tables allow precise dating of these levels. In addition to their use as reference levels for precise determination of vertical throw, paleo-shorelines can provide piercing points for measuring strike slip. As the DSR is leaky in the south and restrained in its central (Lebanon) section, contrasting styles of slip partitioning are displayed.

Slip partitioning in a restraining setting is manifested in the coastal marine and offshore Lebanon work (Elias et al. 2007). Sonar images of the bottom revealed fresh scarps in the soft sediment associated with a >100 km long trace of a the Beirut thrust that is partitioned from the Yammouneh transform segment in the rift (Fig. 8.4). Abrupt emergence of a vermetid reef by ~0.8 m has been dated to the sixth century CE and attributed to the 551 CE earthquake (Morhange et al. 2006). Geomorphic similarity of three successively higher benches suggests a recurrence of a similar M ~ 7.5 event every ~1.6 kyear, since the Holocene sea level maximum (Elias et al. 2007).

Slip partitioning in a leaky setting is evident in the Gulf of Eilat-Aqaba (Deves et al. 2011). Makovsky et al. (2008) have demonstrated that slip is partitioned between the western boundary normal fault (Eilat fault) and a parallel fault that accommodates much of the strike-slip (Avrona fault) (Fig. 8.12). The details of the seismotectonic history of the northern gulf are yet to be resolved. Shaked et al. (2004, 2011) inferred catastrophic submergence for a reef flat in the northernmost Gulf of Aqaba (Fig. 8.12). The seemingly truncated reef table is 4–5 m deep, covered with a few decimeters of sand. Most notably, loose blocks of basement rocks, up to 50 cm in dimension, are laid in a plan similar to archaeological nomadic sites on land (Avner 1998; Avner et al. 1994) (***NS*** in Fig. 8.12). Such loose blocks get carried away by seasonal southern storms at bottom depth of up to 2 m, so the persistent arrangement in a plan reminiscent of archaeological sites indicates fast, perhaps catastrophic submergence. A support for catastrophic events associated with submergence was unearthed onshore: a buried reef with corals in living position, preserving fine skeletal details without any bioturbation or reworking, topped by an unsorted conglomerate (***ET*** near Elat fault in Fig. 8.12). The buried reef preserved evidence for an abrupt sedimentation event ~4.7 ka and a terminal event associated with subsidence and massive sedimentation at ~2.3 ka. A ~4 m vertical displacement is suggested by the submerged reef table (Shaked et al. 2004). At least 2 m and likely the entire 4 m were catastrophically thrown, corresponding to M7¨ ± 0.5 (Wells and Coppersmith 1994). For comparison, trenches in the fan of Sh'horet Creek (Fig. 8.12, ***ST***) reveal 0.1–1.3 vertical displacement events during the same period (Amit et al. 2002). The difference may signify the transition from the Arava/Araba valley to the gulf, yet it may also be related to the difference of seismic response between fan deposits and coral beach.

Additional dating of coral terraces, together with dating turbidites in the deep facies of the Gulf of Aqaba, might complement the history of earthquakes in the southernmost segment of the Dead Sea rift. Efforts to date such deposits are on the way. A control for earthquake dates is provided by Thomas et al. (2007) who report seven archaeological layers damaged by earthquake faulting (some subsequently repaired) since the second century CE. They conclude that historical catalogues are incomplete in this region.

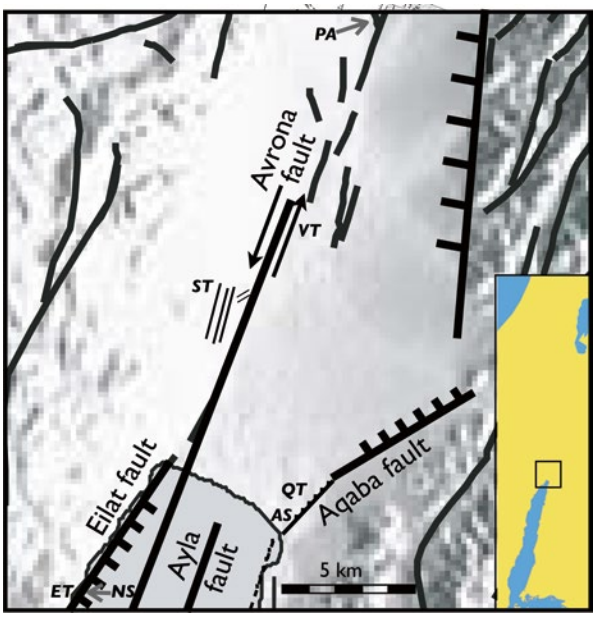

Fig. 8.12 The tectonic setting of the southern Arava/Araba Valley and northern Gulf of Aqaba. The background topography and the curving faults are from Kesten et al. (2008.) Eilat Fault (Modified after Garfunkel et al. 1981). Shaked et al. (2004) have trenched Holocene marine sediments (***ET***) that together with a submerged nomadic site (***NS***) constrain vertical coseismic slip of 4 m ~2.3 ka. The plate boundary northward was mapped by Garfunkel et al. (1981) and strike slip was established based on observation of a small pull-apart basin (PA) when this concept was quite young (Zak and Freund 1966). Holocene sediments crossing this segment, renamed Avrona fault after a playa carrying this name, were trenched by Amit et al. (2002) (***VT***). They report trenching of Pleistocene sediments cut by nearby marginal normal faults (***ST***). Zilberman et al. (2005) surveyed an irrigation system from early Islamic times that was deformed co-seismically during the 1068 CE March event. Makovsky et al. (2008) have identified this fault in the gulf and established left lateral motion of ~30 m on a submerged reef terrace at ~65 m depth. Using this beach line as a piercing point and eustatic curves with estimated age of ~11 ka they inferred a strike slip rate of 2.7 ± 0.5 mm/year. Slater and Niemi (2003) trenched Holocene sediments across Aqaba fault (***QT***). Thomas et al. (2007) have analyzed the adjacent archaeological Ayla sites (***AS***) and identified seven damaged layers, attributing them to earthquakes. Some of the layers show faulting, and some walls record minor strike slip. An earthquake following 360 CE was identified with the 19 March 363 CE event. Tibor et al. (2010) have collected multibeam bathymetric data and verified Makovsky et al. (2008) estimate of offset submerged reef terrace. They have also identified a conspicuous lineament splitting the northern gulf (Ayla fault)

In addition to the direct effect of the Dead Sea rift on the tongue of the Red Sea in the Gulf of Aqaba, and the effect of the Beirut thrust that branches from the rift, earthquakes from the rift affect the entire continental slope of the Mediterranean (Fig. 8.1). Slumps triggered by DSR earthquake show on the bathymetry of the Mediterranean shelf and slope (PS, Fig. 8.8) and seem to generate local sea waves on the Mediterranean coast (Almagor and Garfunkel 1979; Ambraseys and Melville 1988; Ambraseys and Synolakis 2010; Salamon et al. 2007, 2011). Elias et al.

(2007) argue that, for the Lebanese coast, tsunamis are generated by submarine thrusting. High energy deposits in the port of Caesarea (Fig. 8.3), together with destruction of the port, have also been associated with a remote DSR earthquake – the 115 CE event (Fig. 8.2c) (Reinhardt et al. 2006). A sea wave in Yavne was reported for this earthquake (Fig. 8.2a) (Ambraseys et al. 1994). A strong earthquake at Antioch was reported for the same year (Guidoboni et al. 1994). The likely mechanism for sea waves generated by an earthquake rupturing the northern DSR is submarine slumping.

8.2.5 Damage Recorded in Hard Rock

Earthquake shaking often shifts suspended rock masses so they can fall and activate a geological clock. Calcite precipitated in caves, if containing sufficient radioactive Uranium, provides such a clock. Free slope rock falls may become clocks if they contain minerals useful for cosmogenic and luminescence dating, or if they bury such minerals. Indirect clocks can form by modification of the local drainage and accumulating of sediments behind fallen rocks or slides. Researchers of the Dead Sea rift have used all these instances in the quest of dating paleo-earthquakes and assessing their magnitudes.

8.2.5.1 Cave Deposits (Speleothems)

Cave deposits are potentially a useful recorder of ground shaking. The cave protects the deposits from much of the variations in the external environment, and speleothems often show fine lamination, enabling high resolution sampling for dating and for reconstructions of the physico-chemical conditions. In cases where the deposits are datable with sufficient resolution, and deposition is continuous, damage due to earthquakes can be dated. The optimal climate zone for this study should be sufficiently humid to prevent desiccation and sufficiently warm to prevent freezing. The Judean Hills, abutting the Dead Sea rift, proves ideal for the development of this method: deposition in caves is continuous through the dating range of the U-Th method (Bar-Matthews et al. 2000). This has motivated Kagan et al. (2005) to study two adjacent caves in the Judean Hills (Fig. 8.8, SH), where they have documented preferred orientation of severed stalagmites. They have argued that north–south and east–west dominant orientations of fallen stalagmites is consistent with westward propagating surface wave fronts, where the respective polarization of Love and Rayleigh waves would accord with the orientations of fallen stalagmites. Kagan et al. (2005) seem to be the first to present an extended archive of earthquakes based on cave deposits, spanning the last 185 kyear. They have identified 38 datable speleothems seemingly damaged by earthquakes ("speleoseismites"), most of which showing micro-stratigraphic evidence of renewed calcite precipitation following damage. Such evidence together with dating laminae predating and postdating the damage,

bracket the age of damage. Some samples could not be bracketed from both ends, but belonged to clusters of ages; these clusters where taken as a limit for the age of an event. Because Kagan et al. (2005) dated the last damaging event to around 5–6 ka, they inferred that these pre-historic earthquakes were stronger than any historic event.

Braun (2009) has studied Denya Cave in Haifa (Fig. 8.8), a city straddling the Carmel fault (Fig. 8.4). This active branch of the Dead Sea rift bounds the Jezre'el Valley from south (Fig. 8.1). The fault runs closest to heavily populated areas, yet the maximum magnitude expected from the fault and the recurrence rates are poorly constrained. Braun (2009) has devised an isochron method for mitigating sensitivity to the anomalous initial isotope ratios in samples from this cave.

Kagan (2011) and Braun et al. (2011) combined results from the two speleoseismic sites to assess coupling between the Carmel branch and the main Dead Sea rift during the Holocene. They find that the last event to have been well recorded in the Judean Hills, around 5 ka, is the ultimate at Denya Cave, Haifa. The penultimate event hit the two sites respectively at 8–9 ka and 10–11 ka. The authors then use these examples together with data from the Tell Megiddo (Marco et al. 2006) and from the rift valley to lay out possible scenarios for coupling between segments and branches of faults.

8.2.5.2 Free Slope Failure

As in other active regions (McCalpin 2009), landslides and rockfalls in the Dead Sea rift have been used to constrain dates and intensities of seismic shaking. Recently, Katz et al. (2011) have studied landslides triggered by large earthquakes along Ha'Onn Escarpment (Fig. 8.8), east of Lake Kinneret (Sea of Galilee). Measuring optically simulated luminescence (OSL) of buried quartz sand they obtain the following dates for land sliding events: before 65 ka, around 65 ka, 6 ka, and 5 ka. In addition, paleoseismic trenching yielded the following OSL dates for earthquake ruptures: 45, 40, 35, 10, 5 ka, and a younger (<5 ka) event. The 5 ka slide was likely triggered by the earthquake rupture observed in the trench. This work followed Yagoda-Biran et al. (2010) who calculated peak ground accelerations of 0.15–0.5 g required for mobilizing three slides around Lake Kinneret.

Katz and Crouvi (2007) have considered the effect of foundations in ancient settlements: they found that the town Safad/Zefat (Fig. 8.2a) that has been inhabited for more than two millennia, suffers from reduced stability of foundations. Buildings founded in archaeological debris are more susceptible to landslides induced by earthquakes and to amplification of ground shaking. The authors caution that sites like Safad, having been demolished by numerous historic earthquakes, might have biased the historical catalogues towards high magnitudes.

Wechsler et al. (2009) have described a landslide that displaced archaeological remains including an aqueduct in Umm-El-Qanatir, east of Ha'Onn Escarpment (Fig. 8.3). They attribute the damage to the 749 CE earthquake based on the in-site finds limited to sixth to mid-eighth century CE. All these studies manifest the role of earthquakes in triggering land sliding around Lake Kinneret.

A novel approach to earthquake driven gravitational collapse on slopes is given by Matmon et al. (2005). They use cosmogenic dating together with OSL for dating collapse of several meter large sandstone boulders in Timna (Fig. 8.8). They identify three distinct events around 3–4.5 ka, 15 ± 1 ka, and 31 ± 5 ka respectively. Notably the oldest event recorded is associated with a ~5 m boulder displaced 20 m horizontally from its source cliff, with merely 2 m vertical drop. The boulder is found due north of its north-facing scar, suggesting a significant role of horizontal acceleration parallel to the slip vector. Matmon et al. (2005) point out that the cycle of boulder shedding off the cliff may be limited by either of the steps: undercutting and ground shaking. The apparent cycle of 12–15 ka may be determined by the rate of undercutting after a large earthquake. On the other hand, a similar period (yet with a different phase) seems to emerge from Kagan et al. (2005) cave deposits (discussed in the following section). Further research is required for ruling between these proposed mechanisms for determining the period of boulder shedding events.

8.3 Correlation of Historical, Archaeological, and Geological Evidence

The foregoing sections demonstrate that the DSR stands out in the richness of historical, archaeological, and geological evidence of earthquakes. The availability of these three independent and interdisciplinary sources of paleo-earthquake data in the DSR enable cross tests between individual data sets. As pointed out by several authors, the mutual independency of these sources is not always warranted, and circular reasoning should carefully be avoided (Karcz 2004; Ambraseys 2006a; Thomas et al. 2007; Rucker and Niemi 2010).

8.3.1 Prior to the First Millennium BCE

Kagan et al. (2005) have discussed the correlation of speleoseismites and lake seismites. The possibility to match lake seismites to each of the fewer speleoseismites (during times of deposition of the appropriate facies in the lake) has suggested that the cave acts as a filter recording only very strong events. This is in line with the absence of speleoseismites in the historical period. An event dated to earlier than 5.1–6.3 ka can be correlated with a lake seismite dated ~6 ka by Migowski et al. (2004). The correlation between Judean Hills speleoseismites and Lisan seismites was noted by Kagan et al. (2005). Out of four speleoseismic event in the interval 70–15 ka, one was dated to a time of hiatus in the Lisan formation record (event xv).

Table 8.1 Correlation of selected prehistoric earthquakes inferred from archaeologic sites with geochronologically dated seismites

Range [ka]	Archaeological years BCE	Ruin	Geochr-onol. [ka]	Geological site	Refs. notes
5.9–6	Fortieth century	Ghassul	5.9–6.3	Ein Gedi core	a, b, c/1
5.9–6	Fortieth century	Ghassul	>5.3–6.1	Judean Hills caves	a, b, d
5.0–5.1	End 4th mill.	Megiddo	4.2–5.6	Judean Hills caves	d, e
5.0–5.1	End 4th mill.	Megiddo	4.2–5.6	Denya Cave, Mt. Carmel	e, f
5.0–5.1	End 4th mill.	Megiddo	4.7–5.3	Sea of Galilee – Ha-'On	e, g
4.6–4.7	Twenty-seventh century	Ai	4.4–5.0	Ein Gedi core	b, c/1
4.6–4.7	Twenty-seventh century	Ai	3.7–5.5	Tamar Creek	b, c, h/2
4.2–4.3	Twenty-seventh century	H. Ifdan	4.2–4.0	Ein Gedi core	b, c, i/1
4.2–4.3	Twenty-seventh century	H. Ifdan	3.7–5.5	Tamar Creek	i, h/2
3.3–3.4	~ 1365	Ugarit	3.3–3.5	Ein Gedi core	c, j/1
3.3–3.4	~ 1350	Pella	3.3–3.5	Ein Gedi core	c, k/1
3.1–3.2	~ 1150	Pella	3.0–3.2	Ein Feshkha	c, k/1
3.1–3.2	Twelfth century	Deir'Alla	3.0–3.2	Ein Feshkha	l, l
3.0–3.1	~1050	Timna	3.0–3.2	Ein Feshkha	m, n
3.0–3.1	~1050	Timna	2.0–4.2	Mt. Timna	n, o/3
2.75–2.76	~760–750	various	2.75–2.85	Ein Gedi, Ein Feshkha	c, m, p/1
2.75–2.76	~760–750	Deir'Alla	2.75–2.85	Ein Gedi, Ein Feshkha	c, m, l, p/1
2.65–2.75	~700	Various	2.65–2.75	Ein Gedi, Ein Feshkha	c, m/1
2.65–2.75	~700	Deir'Alla	2.65–2.75	Ein Gedi, Ein Feshkha	c, m, l/1

References: (a) Hennessey (1969). (b) Karcz et al. (1977); Karcz and Kafri (1978). (c) Migowski et al. (2004). (d) Kagan et al. (2005). (e) Marco et al. (2006). (f) Braun (2009); Braun et al. (2011). (g) Katz et al. (2011). (h) Gluck (2001). (i) Levi et al. (2002). (j) Schaeffer (1948); Hanfmann (1951). (k) Bourke et al. (1999); Bourke (2004). (l) Ferry et al. (2011), based on Franken (1992). (m) Kagan et al. (2011). (n) Ben-Menahem (1991). (o) Matmon et al. (2005). (p) Ambraseys (2009); Austin et al. (2000)

Comments: (1) Range calculated from sedimentation rates in Ein Gedi core constrained by radiocarbon dates. (2) Large uncertainty in geochronologic date based on OSL. (3) Large uncertainty in geochronologic date based on cosmogenic nuclides

For the other three speleoseismic events, the uncertainty in dating disallows correlation to individual Lisan seismites, yet they seem to correlate to periods of high recurrence rate (see below in the Recurrence section).

There is little data for correlating prehistorical archaeology with geological observations of earthquake damage (Table 8.1). Migowski et al. (2004) correlated the ~6 ka event with archaeological destruction at the Tells of Ghassul (Fig. 8.3). This is one of a series of destructions from the Bronze Age attributed to earthquakes

(Hennessey 1969; Karcz et al. 1977). The speleoseismic date has also been correlated with a 5.3–5.4 ka breccia layer from Ein Gedi core (Migowski et al. 2004; Kagan et al. 2005).

Braun et al. (2011) correlate the latest speleoseismite in the Carmel cave with damage recorded at Megiddo (Marco et al. 2006). This date – ~5 ka – is common to the Judean Caves (Kagan et al. 2005), the ruins of Ai (Karcz et al. 1977), surface rupture documented south-west of the Dead Sea (Gluck 2001), and lake seismite from Ein Gedi core (Migowski et al. 2004) (Table 8.1).

Migowski et al. (2004) correlate a breccia layer from Ein Gedi core dated 4.7 ka with archaeoseismic damage of Ai (Karcz et al. 1977; Karcz and Kafri 1978). This archaeoseismic event also correlates with ground rupture documented south-west of the Dead Sea (Gluck 2001). The uncertainty of dating this rupture, based on OSL, allows correlation also with earthquake evidence 4.3 ~ 4.2 from Khirbet Hamrat Ifdan in Wadi Araba (Levi et al. 2002).Ferry et al. (2011) cite archaeological reports from ongoing excavations and conclude that an earthquake hit the central Jordan Valley around 4.3 BCE.

Ben-Menahem (1991) assigns the Biblical destruction of Jericho to an earthquake, and notwithstanding the delay of seven centuries in writing the text, he calculates a date of 1560 BC for this event. Ambraseys (2009) notes that the biblical story mentions no earthquake. He rejects the archaeological evidence for the biblical Jericho event for which he adopts a date of ~1400 BCE. A seismite from Ein Gedi core is dated to ~3.3–3.4 ka (Migowski et al. 2004) so, in the absence of positive evidence for contemporary earthquake damage in Jericho, one might conjecture that seismic damage elsewhere has inspired the biblical stories from that era.

Migowski et al. (2004) correlate the seismite dated ~3.3–3.4 ka with an earthquake that perhaps destroyed the fortifications of Ugarit (Fig. 8.3) and was arguably referred to by a contemporary tablet in El Amarna in Egypt and by a letter from Abimilki of Tyre (Schaeffer 1948; Hanfmann 1951; Ben-Menahem 1991).

Nur and Cline (2000) suggest that much of the damage to Aegean and East Mediterranean sites around 1200 BCE is due to a 50-year sequence of earthquakes ("storm"). Incidentally, this time window is one of quiescence in the Ein Gedi core (Migowski et al. 2004).

8.3.2 Tenth to Second Centuries BCE

For the last three millennia it is possible to estimate the extent of rupture of historic earthquakes with the aid of archaeological and geological data. The completeness of this information is improving for each consecutive millennium, and for the first half of this period it is clearly insufficient. Figure 8.13 displays interpreted locations of ruptures based chiefly on historical data, with complementary information from archaeology (gray bars) and Dead Sea lake seismites (stars) as they correlate with the historic data. We mark earthquakes matched to Dead Sea lake seismites in Ze'elim Creek, Ein Feshkha (Kagan et al. 2011), Ein Gedi (Migowski et al. 2004), and Daraje Creek (Enzel et al. 2000). The format follows a preliminary attempt by

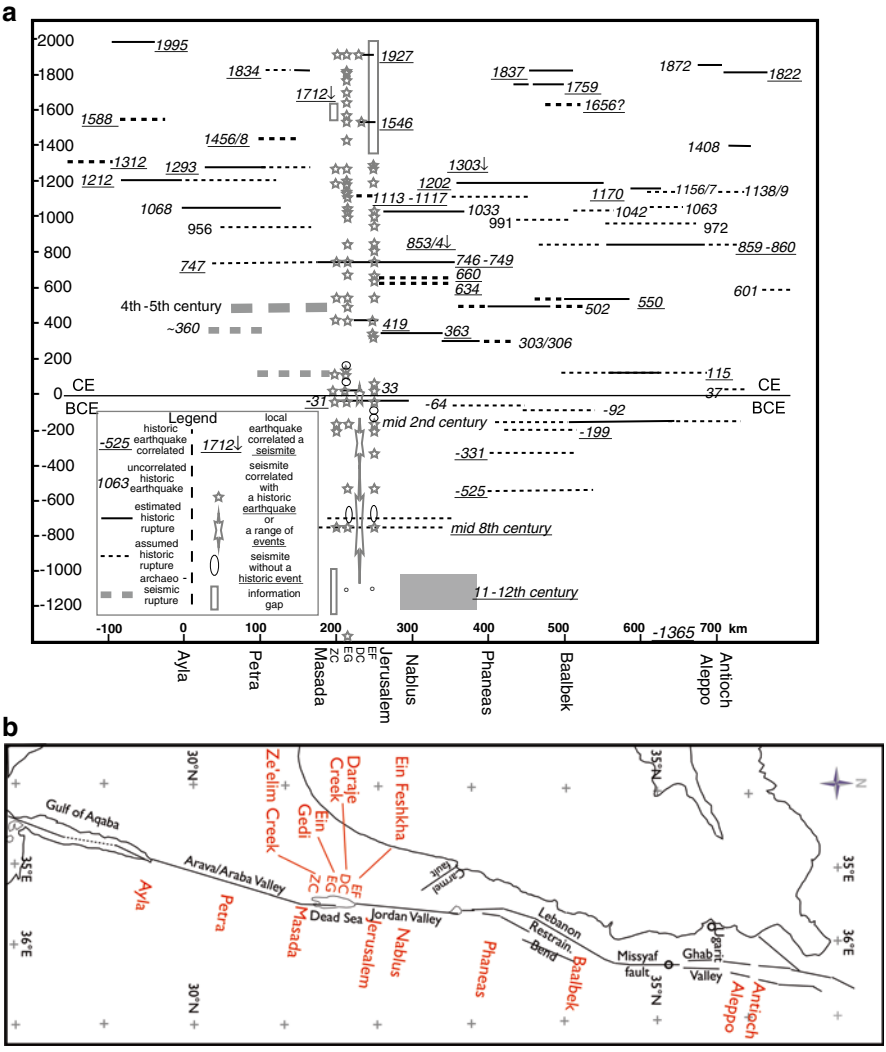

Fig. 8.13 (**a**) Estimated spatial extent of ruptures from the historic periods along the DSR. The extent of rupture (*horizontal lines*) is based on documents and physical evidence. (**b**) Map showing principal archeoseism and paleoseism sites indicated in (a) projected on the main segments of DSR

Garfunkel et al. (1981), which did not have geological data to compare. This update is based on recent catalogues, and includes historical information from older periods, starting with the Biblical earthquake of 759/760 BCE (Guidoboni et al. 1994; Ambraseys 2009). The present version also extends 200 km south-south-west to include the Gulf of Aqaba, where the latest strong earthquake ruptured the DSR: the Earthquake of Nueiba on 22 Nov 1995 amounted to M7.2 or more (Klinger et al. 1999; Shamir et al. 2003; Baer et al. 2008). The interpretation is naturally biased by

the preconceptions of the present author, and it should be taken as a preliminary rather than a definite summary.

As is apparent from the panels of Fig. 8.3 and from Fig. 8.13, the information is sparser for older times and southern locations, in accord with population trends. However, the ability to match a great majority of Dead Sea seismites with historic earthquakes may suggest that the completeness of the historic and seismite archives are not so dissimilar. In this sense, the uneven distribution of ruptures in space and time exhibited in Fig. 8.13 may reflect genuine spatio-temporal clustering of earthquakes in historical times. As Garfunkel et al. (1981) argue, the relative quiescence in Wadi Araba/Arava during the instrumental period supports a different seismic behavior along different segments of the rift.

We start the history of the first Millennium BCE with the earthquake of the mid eighth century as this event is reflected in numerous archaeological sites (Ambraseys 2009). However, note that the Iron Age stratigraphy is being hotly debated, including the role of the earthquake in the cultural transitions (e.g. Herzog and Singer-Avitz 2004; Fantalkin and Finkelstein 2006). Whether all that damage is the result of a single seismogenic rupture remains to be determined. The dates referred to in the Bible enable researchers to name 759 (Ben-Menahem 1979; Ambraseys 2009) as the year of the event. This earthquake is correlated in all three Dead Sea paleoseismic sites (stars in Fig. 8.13). Kagan et al. (2011, Appendix C) point out that each of the three seismite sites exhibits two eighth century events. This is in line with the large areal extent of damaged archaeological sites that led researchers to infer a very high magnitude single event. Austin et al. (2000) assign M8.2 to this earthquake. Ambraseys (2005a) notes that such a high magnitude earthquake would completely demolish Jerusalem, where historical or archaeological evidence for destruction is not established.

The assumption of a regular repeat time of a century for Dead Sea earthquakes is central to the Austin et al. (2000) argument. And indeed, a superficial inspection of the catalogues for the last millennium can yield an approximately uniform rate of repeat times for destructive earthquakes in the Holy Land, namely once a century. However, a closer look shows pairs of events that often span a wide section along the transform. Salamon (2010) has reviewed sequences of historic earthquakes and identified 13 cases where successive events did not necessarily form as aftershocks. We note two pairs of earthquakes separated by a decade or less: 1202 CE ruptured Lebanon, severely shaking Syria and northern Israel; 1212 hit the Gulf of Aqaba. These events with magnitudes estimated 7.0–7.5 could erroneously be taken as a single $M>8$ event if we did not have the temporal resolution. The pair of 1834 CE ($M\sim6$) and 1837 CE (M7.0, Ambraseys 1998) at the Jordan and Dead Sea Valleys and Lebanon, respectively, would be taken as a single $M\sim7.5$ event.

In addition to the unjustified assumption of a century long seismic cycle, criticism of Austin et al. (2000) comes from archeological grounds. Fantalkin and Finkelstein (2006) argue that some of the damage purported to originate from seismic shaking could have resulted from static loads.

The successive seismite found in Ein Gedi core (Migowski et al. 2004) and at Ein Feshkha (Kagan et al. 2011) is correlated to 525 BCE. This earthquake is listed by Ben-Menahem (1991) and Sbeinati et al. (2005), with damage to the southern

Lebanese towns Sur and Sidon, and a local sea wave. Morhange et al. (2006) document variable uplift of paleo-shore-lines from this period, and suggest multiple seismic events. The 551 CE event, with perhaps larger macroseismic effects, (Elias et al. 2007) is recorded as well at both these seismite sites, yet in addition it is correlated to a seismite at the southern (further form the epicenter) Ze'elim Creek site. The fact that 550 BCE is not correlated in Ze'elim Creek may be due to a smaller source, or due to less favorable sedimentary conditions (e.g. lack of lamination) in this particular interval. Additional studies in a lake-ward section, being exposed due to the ongoing level drop, may resolve this issue.

The three overlying clear seismites in Ein Feshkha (Kagan et al. 2011) were not correlated, largely due to sparse historical evidence from that period (deformed layer is considered "questionable"). The correlation of an overlying seismite to 331 BCE in Syria is based on a nineteenth century chronicle ("many victims and destruction") interpreted by Sbeinati et al. (2005) as intensity $I = VI$. Enzel et al. (2000) date a seismite from Daraje Creek to 2.0–2.4 ka, correlative with the 331 BCE Ein Feshkha seismite, or with one of the adjacent uncorrelated seismites.

Two additional seismites at Ein Feshkha are uncorrelated between 331 and 199–198 BCE, yet the error in dating could allow respective correlation with the adjacent seismites. The latter date corresponds to a damaging earthquake in the southern Lebanese coast, with more than half of Sidon destroyed by a landslide, for which Guidoboni et al. (1994) and Sbeinati et al. (2005) respectively assign intensity *X* and *VIII*. This event was not recorded in Ein Gedi core and Ze'elim Creek.

Of the 30 deformed layers in Ein Feshkha section overlying the one correlated to 199–198 BCE, spanning second century BCE to fourteenth century CE (the sequence is truncated), three are labeled "questionable" seismites. All 30 deformed layers could be matched with historic earthquakes to within he dating error (Kagan et al. 2011). While each individual deformed layer can be matched to one or several earthquakes, a unique match of the entire set is not possible: the best fit Bayesian model of radiocarbon ages anchored to historic earthquakes (Kagan et al. 2010) leaves 2 out 30 seismites unmatched at respective model dates (95 % confidence) of 101–42 BCE and 365–595 CE (the latter considered "questionable").

Except for the last century in this sixteenth centuries long interval, the Ein Gedi core is particularly detailed as it corresponds to the chronologic model based on laminae counting anchored to 22 seismites (Migowski et al. 2004). Two of these are not matched to historic earthquakes, at respective model dates of ~90 and ~175 CE. Note that the two pairs of unmatched events in from each section considered are not correlated mutually, suggesting four local shocks that were not recorded historically.

Several earthquakes from the counted laminae interval are worth noting. These are large historical events that are expected to affect the Dead Sea basin.

The information about a mid-second century BCE events is scant and comes from secondary but relatively reliable sources. Several dates between 148 and 130 BCE are mentioned in the sources, and the confusion is yet to be resolved (Ambraseys 2009; Guidoboni et al. 1994; Karcz 2004; Sbeinati et al. 2005). Significant destruction of the city of Antioch was reported (Guidoboni et al. 1994; Ambraseys et al. 1994; Guidoboni and Comastri 2005; Sbeinati et al. 2005; Ambraseys 2009). Historical accounts cannot

distinguish between a Dead Sea rift source and adjacent plate boundaries. A tsunami hit the Lebanese coast near Sidon. A collapse of a village "above Sidon" (Karcz 2004, and historical sources therein) suggest ground shaking and a regional earthquake. For a single event to be responsible to the damage from Antioch to Ptolemais, some 400 km (Fig. 8.2), it should be M ~ 8. Yet a pair of events, each around M7.5, is consistent with the geological data (Kagan et al. 2011) and with the historical evidence for two separate earthquakes. Ze'elim Creek and Ein Gedi core feature each a seismite from the mid-second century BCE (Migowski et al. 2004; Agnon et al. 2006; Kagan et al. 2011). Ein Feshkha section features two clear seismites from that time, separated by a 4 cm undisturbed sequence. The calculated mean rate of deposition – 0.27 ± 0.03 cm/year, yields a minimum of 13–17 years between events. Including an additional 1 cm of sequence embodied in the upper seismite would give 17–20 years. This is similar to the upper range of difference between various interpretations of historic dates.

8.3.3 First Century BCE to Seventh Century CE

A regional earthquake is reported for 92 BCE with tsunami in Lebanon and flooding in Egypt, but its source location is not clear. This event is correlated to seismites in Ein Feshkha and in Ein Gedi core, while Ze'elim Creek sections show undisturbed laminar facies. We will use this information for a comparison with more recent events for which we have more information.

The 64 BCE earthquake was studied in detail by Karcz (2004). He concluded that "it is unlikely that local intensity was much in excess of human perception". Sbeinati et al. (2005) have reevaluated this event (65 BCE) and classify the completeness of data as "acceptable". An intensity VI is assigned to Jerusalem, where the source is likely in western Syria (*VIII* > *I* > *VII* in Antioch). While Ken-Tor et al. (2001) identify this event with a seismite in Ze'elim Creek, Agnon et al. (2006) preferred a mid-second century source for that seismite. They based their correlation on a deposition model with a uniform sedimentation rate except in hiatuses. Accepting this model, the 64 BCE event would be reworked and "masked" by the subsequent 31 BCE earthquake. Migowski et al. (2004) were the first to acknowledge that the subsequent 31 BCE event would mask 64 BCE. Recently however, Kagan et al. (2011) have found a seismite at this period in the Ein Feshkha section, in agreement with Sbeinati et al. (2005) intensity assessment. If we are to accept Karcz' (2004) assessment that the Syrian earthquake was only felt around the Dead Sea, we miss a local event during that period that left a mark on the Dead Sea sediments, and perhaps was erroneously amalgamated with the large 64/65 BCE earthquake that hit Antioch.

The 31 BCE and the subsequent 33 CE earthquakes are well known due to their contemporaneity with dramatic political and military events. Kagan et al. (2011) classify these earthquakes as two of the nine forming "intra-basin seismites", identified in the three sections considered in detail. In addition, a seismite dated ~2 ka in Daraje creek (Enzel et al. 2000) could be correlated to one of these earthquakes.

The 362/363 CE earthquake deserves special attention, as since Russell's (1980) work it is considered one of the largest events on DSR (e.g. Ambraseys 2009). Kagan et al. (2011) suggest that two events of M ~ 6.5, one from 363 north of the Dead Sea and one from a close date south of the Dead Sea, had been erroneously amalgamated to a single M > 7 event. The sites north of the Dead Sea are skewed significantly to the west, suggesting a Carmel Fault source. The Seismite C in Ze'elim Creek section of Ken-Tor et al. (2001) was constrained by radiocarbon dates to correlate with either the 363 or 419 CE earthquake. A uniform deposition rate model of Agnon et al. (2006), anchored to historic earthquakes, ruled in favor of the latter date. Likewise, an Ein Gedi core seismite from the laminae counting interval was correlated with 419 CE, where 363 CE was not correlated (Migowski et al. 2004). Kagan et al. (2010, 2011) section in Ze'elim Creek was fit better to models with a seismite from 419 CE, where again 363 CE was not correlated. By contrast, their models for Ein Feshkha section show correlation of seismites to both earthquakes. They suggest that the Ein Feshkha records a moderate earthquake that hit the north, whereas the southern earthquake did not generate seismites in the study sites. A single large earthquake that demolish the entire region from the Galilee to Petra and Aila would correspond to M7.4 (Ambraseys 2006b, 2009; Russell 1980; Thomas et al. 2007). This would result in broad scale damage on the east of the rift, in contrast to the observations (Russell 1980). Kagan et al. (2011) interpret the historical and the physical observation as a pair of consecutive smaller events, one in northern Israel (perhaps on the Carmel fault) and one in the Arava/Araba Valley. This issue requires additional research.

The earthquake of 419 CE, generating "intra basin seismites" according to Kagan et al. (2011), is likely a local moderate event. The limited reports of damage do not allow a precise location of source, but it may be similar to 1927 Jericho M6.2 earthquake. By contrast, the 551 CE earthquake that is also considered by Kagan et al. (2011) an "intrabasin seismite" is a remote and strong event: it ruptured a putative thrust under Lebanon with an estimated M ~ 7.5 (Elias et al. 2007).

Rucker and Niemi (2010) speculate that a strong earthquake hit east of the Dead Sea 597–598 CE, based on an inscription in Areopolis. Since historic documentation from Petra is missing after 597 CE, such an event might have escaped the chronicles. Ambraseys (2009) also lists an earthquake earlier than 597 in Areopolis. Hence the correlation of all sixth century seismites with the Lebanon event is still not certain.

The Jordan Valley has been struck by three earthquakes during the seventh century CE: one at 634 and two at 660 (Amiran et al. 1994; Guidoboni et al. 1994). Tsafrir and Foerster (1997) dated earthquake damage in Scythopolis/Baishan to between the end of the sixth century and the second half of the seventh. Additional archaeoseismic evidence was reported nearby in Ein Hanatziv (Karcz et al. 1977). Kagan et al. (2011) found two seismites in Ein Feshkha, while a laminated sequence was deposited in Ze'elim Terrace. Migowski et al. (2004) correlated the single seismite from Ein Gedi core with the latter year. This is consistent with northerly local sources, and a stronger shaking in the Dead Sea from the 660 event that is said to had been strong at Jericho (Amiran et al. 1994).

The high resolution of late Holocene sequences exposed during the recent retreat of the Dead Sea lake is used by Neumann et al. (2009) for assessing possible geobotanic response to large earthquakes. They have investigated the Ein Feshkha section, exposed on the north west corner of the lake (Fig. 8.7), and found inconclusive evidence for possible seismic effects on olive pollen.

8.3.4 Eighth Century CE

Karcz (2004) and Ambraseys (2005a) studied the historical sources of this period and suggest that damage reports for a 749 CE earthquake were accentuated by confusion with an earlier event (~747 CE); amalgamation of these two (and perhaps more) events gave an overestimation of the size of the 749 CE event. The mid-eighth century CE events have been reportedly recognized in a number of additional sites (Marco et al. 2003). The assignment of the spectacular parallel pair of fallen colonnades of a Byzantine church in Hippos (Fig. 8.6c) to the 749 CE event (e.g. Nur 2008) is not based on archaeological evidence. A fallen colonnade from another Byzantine church on the site can be tied to the mid-eighth century events, based on an inscription from the late sixth century CE on one of the columns (Fig. 8.5d) (Marco 2008; Segal 2007). In any case, such spectacular manifestations of ground shaking may be misleading in that they strongly depend on the masonry, and the information they give on ground motion turns out to be limited (Hinzen 2011). The above mentioned earthquakes during the seventh century CE, while less famous, can be associated with the Hippos damage.

Kagan et al. (2011) report two seismites from the mid eighth century. This may seem consistent with a pair of earthquakes at Jerusalem at 746 and 757 CE, reportedly damaging Al Aksa mosque (Ambraseys 2009). However, their correlation hinges on the assignment of the underlying seismite to 873 CE discussed below.

The rupture in Qasr Tilah trenched and dated seventh to tenth century CE by Haynes et al. (2006) could be associated with a mid eighth century event. Support to this hypothesis is given by Bikai (2002) and Eklund (2008), who infer terminal destruction of Petra due to an earthquake at the mid eighth century.

8.3.5 Ninth to Eleventh Centuries CE

This period is marked by the transition of the center of the Muslim empire from Damascus to Baghdad, and a consequent deterioration of the quantity and quality of chronicles. This is evident in the confusion regarding some of the earthquake reports from the period, and in particular for the years 873, 956, and 1068 CE. Despite becoming a periphery, the Levant is mentioned in numerous earthquake reports (Ambraseys 2009). During this period the Ein Feshkha paleoseismic sites show high rate of activity, and it is difficult to identify individual events.

853/4 CE: An earthquake with dramatic mass movements and tragic consequences had been recorded in Tiberias and vicinity (Sbeinati et al. 2005; Ambraseys 2009). This event is likely recorded in one of the numerous seismites from this period, yet no particular correlation has been suggested (Table 4 of Kagan et al. 2011).

873 CE: The historical evidence originated from well within the Arabian Plate (Ambraseys et al. 1994; Ambraseys 2009). Haynes et al.'s (2006) conjecture that this earthquake originated from a surface rupture at Qasr Tilah constrained to between the seventh and tenth centuries. In order to accept this conjecture, we need to accept that "due to the sparse population of the Hejaz and Wadi Araba, the historical record of the earthquake maybe distorted or biased, thus the catalogue may be incorrect". As suggested above, the Qasr Tilah rupture might be associated with one of the mid-eight century events. Kagan et al. (2011) tentatively identify the 873 earthquake in the northern (Ein Feshkha) and central (Ein Gedi) sections of the Dead Sea, but not in the southern (Ze'elim Creek) (Fig. 8.13). Barring directivity effects, this could indicate a lower sensitivity of the southern site. More likely, and considering the historical indications for a remote source, the 873 event is not recorded in the Dead Sea.

Tenth century: Only a few seismites are apparent in the sections correlated to the tenth century: two in Ein Feshkha (Kagan et al. 2011) and one in Ein Gedi (Migowski et al. 2004). Likewise, only a few earthquakes appear in historical catalogues covering that period in the Levant (Sbeinati et al. 2005; Ambraseys 2009). As pointed out by Ambraseys (2009), the earthquakes of 952 (on the junction of the DSR with EAF) and 956 (Eastern Mediterranean with damage in Egypt) had been confused by a contemporary chronicler. The single seismite identified in Ein Feshkha at the mid-tenth century (Kagan et al. 2011) reflects one of these large events or a smaller one not recorded historically.

1033 CE: This event ruptured the surface in the Jordan Valley and had been designated $7.0 \leq \mathrm{Ms} < 7.8$ (Ambraseys and Jackson 1998). More recent work excluded that earthquake from the set of $\mathrm{Ms} \geq 7.0$ events on the DSR (Ambraseys 2009). Ferry et al. (2011) associate the ultimate rupture trenched in the Jordan Valley with this event, reasserting that this is one of the largest historic earthquakes recorded on this segment. Migowski et al. (2004) identify a 7.4 thick breccia layer with the 1033 CE earthquake, for which Kagan et al. (2011) correlate a 1.5 cm seismite. The absence of a seismite report from Ze'elim Creek may be due to sandy facies and difficult access.

1063 CE: Significant damage in Tripoli (VII-VIII, Sbeinati et al. 2005) led Elias et al. (2007) to infer rupture on a local fault that they mapped traversing the coast and bounding the Lebanon Thrust from north. A rupture of the entire mapped length, 65 km, would generate $\mathrm{M} \sim 7$ earthquake, which is a likely upper bound for this earthquake. Such a magnitude would be consistent with Eq. 8.3 and the systematics of Wells and Coppersmith (1994). This earthquake is correlated to a seismite in Ein Feshkha. Migowski et al. (2004) considered this earthquake to be masked by the subsequent 1068 CE earthquake. However, using the resolving power criterion of Agnon et al. (2006), it seems that this earthquake might be resolved in case that it generated

a seismite: the 1068 seismite is only 4 mm thick; the resolution for this thickness varies between 2 and 5 years during the time between the eighth and thirteenth centuries. If the absence of a seismite in the laminae counting interval in Ein Gedi core can be corroborated in nearby sections, it can be used for calibrating the attenuation relation as discussed below. Yet this potential can be realized only if it can be shown that no small, local, and forgotten event is responsible for the Ein Feshkha seismite.

1068 CE: The latter earthquake was also identified with archaeological damage in the southern Arava (Zilberman et al. 2005). These authors detected vertical displacement of up to a meter across an early islamic irrigation system. Using accepted magnitude – rupture length – slip systematics (Wells and Coppersmith 1994), Zilberman et al. (2005) suggest an $M > 6.6$. Accepting that the rupture extended to Qasr Tilah, about 150 km to the north, this earthquake could have reached M7.2–7.8 m, consistent with several m average lateral slip. The event is recorded both in Ein Gedi core (Migowski et al. 2004) and Ein Feshkha, where the Ze'elim Creek sections are in sandy facies with difficult access (Kagan et al. 2011).

8.3.6 Twelfth to Fifteenth Centuries CE

Historically, this period from the Crusades to the Ottoman conquest is very well represented by chroniclers from both the Frankish and the Muslim cultures. Historical records of seven large earthquakes found in catalogues are correlated to Ein Feshkha seismites (Kagan et al. 2011): 1114/1117, 1150, 1170, 1202, 1212, 1293, 1312. Of these, four are correlated in the laminated section of Ein Gedi core (Migowski et al. 2004; Agnon et al. 2006): 1114/1117, 1202, 1212, 1293. Only two thirteenth century events are correlated in Ze'elim Terrace (Kagan et al. 2011, following Ken-Tor et al. 2001). The southward diminishing abundance of seismites may reflect the observation that the historic earthquakes from the twelfth and fourteenth centuries ruptured north of the Jordan Valley (Ambraseys 2006a, b, 2009; Sbeinati et al. 2005). The 1202 CE event is a special case: it was very large ($M \sim 7.5$) and closer to the Dead Sea than the earthquakes from adjacent centuries. Also, 1202 is so close in time to 1212 that the two seismites are not always resolved from each other (Agnon et al. 2006). So a generalization may be made that large earthquakes from north of the Jordan Valley may be sufficiently intense at the north of the Dead Sea to generate a seismite, but the intensity decays significantly to the south of the lake. We use this observation in calibrating the attenuation relation below.

8.3.7 Sixteenth to Nineteenth Centuries CE

This period is not represented in the Ein Feshkha section due to local truncation, and future work on nearby outcrops can fill this gap. Ein Gedi core shows eight seismites correlated to the historic earthquakes of 1456/1458, 1546, 1588, 1868, 1712, 1759,

1822, 1834/1837. Ze'elim Creek shows a 10 cm thick seismite for the first and a 25 cm thick one for the last of these events (Kagan et al. 2011). The facies in the sixteenth-seventeenth centuries of this site does not allow rejection of sedimentary disturbance. Yet the eighteenth to early nineteenth centuries left a laminar and undisturbed deposit, suggesting that the 1712, 1759, and 1822 earthquakes were not intense there. This is in agreement with the northerly epicenters of these events (Sbeinati et al. 2005; Ambraseys 2009).

A comment on 1546 CE: As mentioned above, Enzel et al. (2000) have identified the topmost liquified layer in Daraje Creek with the instrumental 11 Jul 1927 M6.2 Jericho earthquake. Ambraseys and Karcz (1992) note that the 1546 earthquake was similar in damage distribution to the 1927 event, so the penultimate rupture in Daraje Creek (dated mid-2nd Millennium CE) could arguably associated with this rupture. Kagan et al. (2011) assign both earthquakes to the Kalia fault that traverses the basin some 20 km north of the Daraje Creek rupture. Yet it is not inconceivable that the ruptures recorded in the fan delta are of large aftershocks: a M6.2 event typically triggers aftershocks up to M5.2. Wells and Coppersmith (1994) give this as the lower limit for breaking the surface by normal faults, with rupture lengths of several km. The age of the penultimate event determined by Enzel et al. (2000) is 400–500 years, in agreement with the 1546 CE date of the historic event similar in damage distribution to the 1927 Jericho earthquake (Ambraseys and Karcz 1992). The penultimate Daraje seismite can again be interpreted as an aftershock of a M ~ 6.2 event on Kalia fault. Alternatively, a shore-parallel fault segment in the north-west of the lake was the source for either or both these moderate events.

8.4 Completeness

All the records used by seismologists are incomplete in one or more aspects. Historical, archaeoseismc, and paleoseismic archives have the advantage of going back in time, as compared with the more systematic instrumental archives. However, the non-instrumental archives suffer from inherent problems of completeness. The more complete the archive, the more one can use it as an independent data set to correlate with others.

Historical archives are limited by the availability of cultures writing history and by preservation of these writings. During several periods the Levant was populated by coexisting (often competing) literate cultures, leaving complementary archives that can be mutually cross-checked. This was the case at Medieval times, when Muslim and Crusader historians described the same earthquakes (e.g. Ellenblum et al. 1998; Guidoboni and Comastri 2005) or during the Roman times, for which Roman as well as Jewish sources are available (e.g. Karcz 2004). When the center of the Islamic empire moved from Damascus to Baghdad, during the mid eighth century CE, the reports of earthquakes became vague. This process culminated with the 1068 CE earthquakes. Al-Bana, a contemporary chronicler who lived in Baghdad, reported two events for the same year – 18 March and 29 May. The two

reports are very similar- except that the latter states a complete devastation for Ramla and only Ramla. Makdisi (1956) suggested that Al-Bana got two versions of the same event from two independent sources, where the date records the time of arrival of the report or of its recording in writing. The former report was accurate (an earthquake in the south corroborated by additional sources) and the latter was spurious (devastation of Ramla). Perhaps it confused the more likely devastation of Ramla in the 1,033 event which was confirmed by other sources (Ambraseys 2009). This case exemplifies the effect of political geography, demography, and in particular distribution of literate population. A well known general observation is that the southern parts of the rift, that bisects large deserts, is clearly less represented in the historical archive. Further advance in the use of historical data in seismological research requires a systematic assessment of the completeness of the archives.

8.4.1 Archaeological Archives

Archaeological archives are possibly incomplete due to discontinuous occupation and also due to poor conservation or lack of excavations. For example, Tel Ateret records the 1202 CE earthquake during the Ayyubid times when it was used as a shrine, shortly after the site was constructed by Crusaders and conquered by Saladin (Ellenblum et al. 1998; Ellenblum 2007). Archaeology sets a limit also on the time of the ultimate earthquake: it had ruptured during the Ottoman times, after the introduction of tobacco. This is due to the discovery of smoking pipes on a floor in context with a wall displaced ~0.5 m (Marco et al. 1997; Ellenblum et al. 1998). During that time the site was not occupied, although it was in marginal use as a shrine. Luckily, historical considerations including reported damage could distinguish between 1759 and 1837 CE, and between the two shocks of the former year (Ambraseys and Barazangi 1989; Ambraseys 1998; Ellenblum et al. 1998).

The distribution of archaeological sites during the period of consideration is a key to the potential of retrieving a complete archive. Sparse monumental building during antiquity is reflected by localized evidence for destruction. The Chalcolithic Tells of Ghassul (Table 8.1) are a good example. As has been said for the historical archive, the southern parts of the rift that bisects large deserts is clearly less represented in the archaeological archive.

8.4.2 Lake Archives

Lake archives are limited by hiatuses, not always evident in outcrop (e.g. Machlus et al. 2000), and by facies. When layering is obliterated during diagenesis by turbation (e.g. shallow facies susceptible to wave action) there is no mark of earthquakes. In the case of the Dead Sea, seismites from evaporites such as halite and gypsum

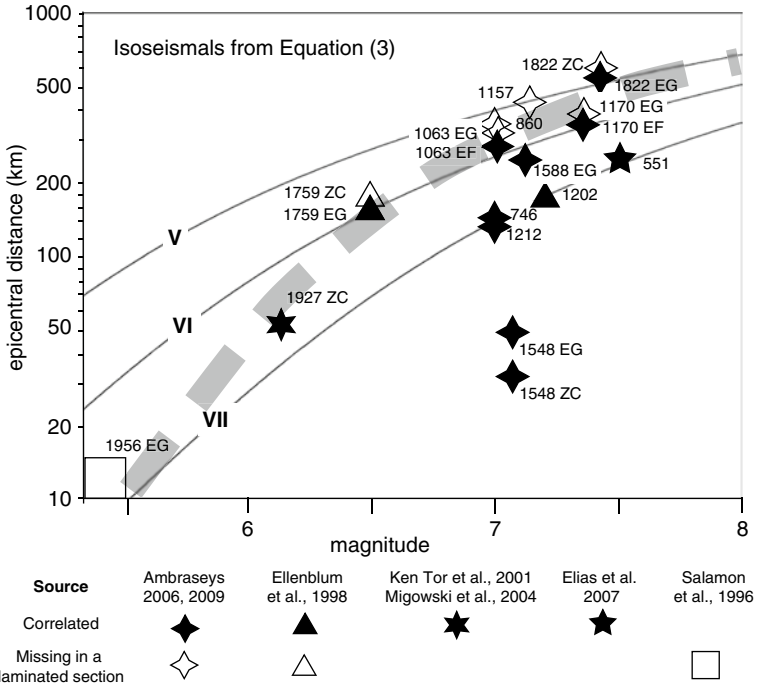

Fig. 8.14 Distances of selected historic ruptures (logarithmic) from Dead Sea seismite sites versus macroseismic magnitudes. The *empty symbols* denote sites without a correlated seismite for a given earthquakes (years CE)

have not been studied. The advantage of lake records is that superposition is dictated by gravity, and layers (down to laminae scale) are continuous and sub horizontal on outcrop scale and larger. Therefore disturbances due to high mechanical energy at lake bottom tend to stand out in outcrop and attract attention.

A method to test the completeness of the lake events during historic periods is presented in Fig. 8.14. The format is familiar from Fig. 8.3, but this time we only plot isoseismals V-VI-VII using Eq. 8.3 (Hough and Avni 2011). We plot individual earthquakes using a solid symbol for those correlated to a Dead Sea seismite, and an empty one for uncorrelated ones. For this preliminary edition we focus on events with better constrained magnitudes and locations, and in particularly on events that are correlated for one of the sites and absent in another. This helps to constrain a hypothetical critical isoseismal for the generation of seismites in the Dead Sea (gray broken curve). The critical intensity required for seismite formation seems to diminish with magnitude and distance: for a close epicenter (<40 km) and small magnitude (≤6) the critical local intensity is close to VII; for a distant epicenter (>300 km) and high magnitude (≥7.2) the local intensity is V-VI. The critical curve in Fig. 8.14 gives a preliminary criterion for the completeness of the lake record.

8.4.3 Cave Archives

Cave archives require special caution with regard to completeness. Limestone precipitation is not regular and the ensuing stratigraphy may be complex. Recently, Kagan (2011) and Braun et al. (2011) have reported a paleo-earthquake in the Judean Hills caves (SH and in Fig. 8.8) at ~8.6 ka. They go on to compare the archive from this site with the Denya Cave site (DH in Fig. 8.8), considered a proxy for activity on the Carmel fault, and with lacustrine and landslide archives. This comparison allows Kagan (2011) and Braun et al. (2011) to discuss coupling of the transform with its Carmel fault branch. For the Pleistocene however, such a discussion would critically depend on the assumption that both records are complete. A complete speleoseismic record will be achieved only at the limit where additional age determinations give no new dates of paleo-earthquakes. Another issue with the present state of the art is that five out of 18 speleoseismites reported by Kagan et al. (2005) had no dated material preceding damage, so they were biased by the use of the *terminus ante quem* as damage date.

8.4.4 Rockfall Archives

Rockfall archives also require statistically significant sampling, such that new sampling adds no new dates. With the present costs of cosmogenic dating, and with the low availability of new techniques such as *in situ* C^{14} dates, this requirement is not realistic, so rockfall archives can hardly be considered complete.

8.5 Discussion: Recurrence Patterns

A chief goal of paleo-earthquake research is resolving recurrence patterns and, in particular, recurrence intervals characteristic of the seismogenic zones in question. Goes (1996) has used historical and paleoseismological records from the American continent to evaluate *aperiodicity* (α) of large earthquakes, using a definition of α as

$$\alpha = \frac{\sigma(\tau)}{\langle \tau \rangle} \tag{8.4}$$

In Eq. (8.1) τ represents the distribution of recurrence intervals, the <brackets> denote average, and σ is the standard deviation. A perfectly periodic behavior is represented by vanishing α whereas clustered behavior yields α larger than unity. Goes (1996) also recognized the limitation imposed by the brevity of archives, one that is alleviated by the long time recorded for the DSR.

Table 8.2 Distributions of recurrence intervals at different locations and times along the Dead Sea rift

Site/segment	Window [ka]	Recurrence interval [kyear]			σ(τ) SDEV	aperiodicity α ⟨	n	Reference
		Mean	Max	Min				
Judean Hills	185–0	9	24.5	3	6.7	0.73		K05, B11
Peratzim Creek	72–25	1.6	8.5	0.25	2.9	1.8	29	M96, A06
Ein Gedi Core	4–0	0.1			0.088	0.9		M04, A06
Ein Gedi Core	2–0	0.05			0.07	0.75		M04, A06
Ein Feshkha	2.5–0	0.05						
Ze'elim Terrace								K11
Dead Sea								
Yammounneh	~12–6	1–1.2			Unknown		5–6	D07
Yammounneh	6–0	1–1.2			Unknown		5	N08
Jordan Valley	25–0	0.79	1.5	0.28	0.52	0.66	5	F11

A06 – Agnon et al. (2006), B11 – Braun et al. (2011), D07 – Daeron et al. (2007)
F11 – Ferry et al. (2011), K05 – Kagan et al. (2005), K11 – Kagan et al. (2011)
M04 – Migowski et al (2004), M96 – Marco et al. (1996), N08 – Nemer et al. (2008)
α "intra basin seismites" (IBSs), simultaneously recorded at Ein Feshkha, Ein Gedi core, and Ze'elim Terrace

The foregoing section clarifies that a discussion of recurrence based on the records we have may suffer from their incompleteness. Yet such a discussion can help point out gaps in the information needed for advancing our understanding of the nature of seismogenic zones. Table 8.2 summarizes data on recurrence from several studies that provide sufficient information for characterizing the distribution of intervals.

Marco et al. (1996) have identified 29 seismites in the dated section of Peratzim Creek and inferred a mean recurrence interval of 1.6 kyear between ~72 and ~25 ka. Agnon et al. (2006) have revised the estimate based on more extensive ages of Haase-Schramm et al. (2004). This age scheme recognized a 5 kyear hiatus in the Lisan Formation around 45 ka (Fig. 8.15). The variation, between 250 and 8,500 years, is a clear manifestation of temporal clustering of earthquakes. More accurate and extensive dating of Lisan Formation will modify the figures (Stein 2011) but clustering of seismites will likely prevail (Kagan 2011).

Figure 8.15 shows the cumulative number of seismites versus interpolated age using Haase-Schramm et al.'s (2004) age model. Anomalous lithology and hiatuses are marked following Stein (2011) who has tabulated the ages versus depth and interpolated for seismite ages. Figure 8.16 shows smoothed recurrence intervals on a logarithmic scale. Despite the periods of poor dating constraints (including hiatus 43–48 ka), Figures 8.15 and 8.16 show a pattern of long quiescence periods between quasi-periodic clusters. During each cluster of seismicity the recurrence interval is quite uniform, varying among clusters between 200 and 1,400 years. Quiescence periods may linger 3–10,000 years.

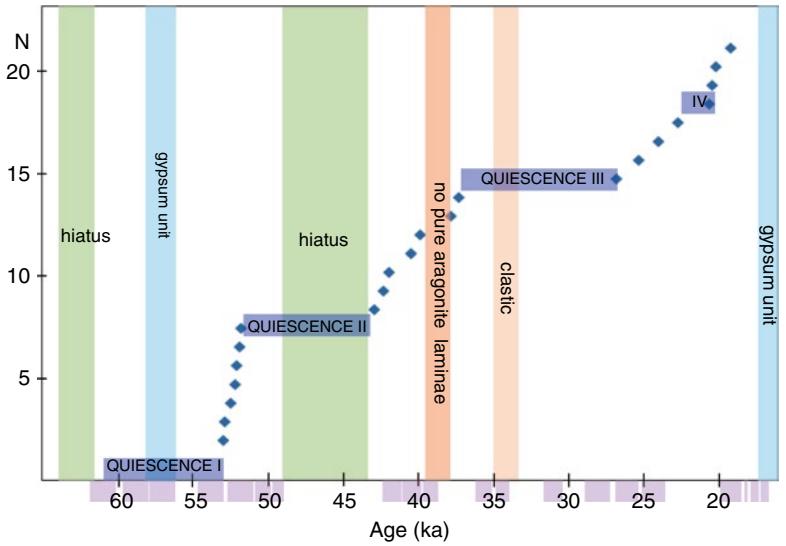

Fig. 8.15 Clustering of seismites in Lisan Formation. The *horizontal axis* shows model ages (Stein 2011) according to stratigraphic heights in PZ1 (Marco et al. 1996) of dated samples (Haase-Schramm et al. 2004). Anchors for the age model are marked by *magenta rectangles* beneath the axis. The *blue diamonds* denote cumulative number of seismites. Periods of anomalous deposition (gypsum, clastics, their aragonite-poor inter-lamination) or lack of are shown by colored shading. Four periods of apparent quiescence emerge separated by quasi-periodic clusters of activity (See Fig. 8.16)

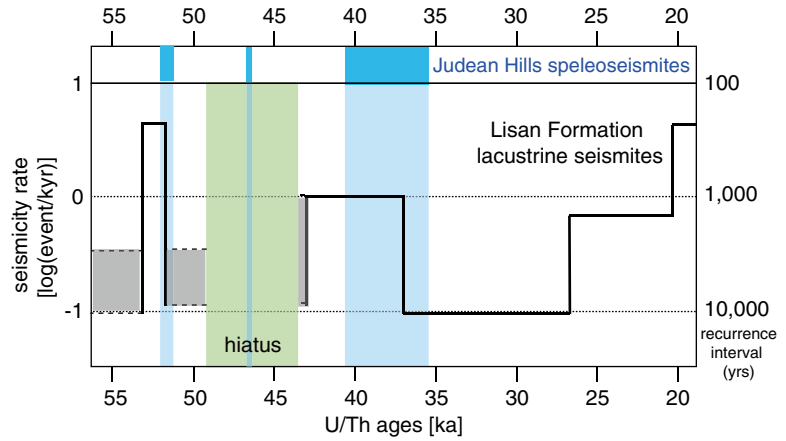

Fig. 8.16 Rates of seismicity recorded in the Lisan Formation and Judean Hills caves. The ordinate gives the logarithmic rate of Lisan seismites (event per millennium; see *right hand axis* for recurrence intervals in years). The *gray rectangles* represent the uncertainty: *upper bound* is calculated based on the intervals represented by continuous deposition of datable sediments; *lower bounds* assume no large earthquakes during non-datable intervals (data as in Fig. 8.15). *Cyan rectangles* represent date ranges of Judean Hills speleoseismites following Kagan et al. (2005). Other colored rectangles as in Fig. 8.15

The high rate of seismicity at ~52 ka (an event in ~200 years) is anomalous for the entire period represented by sediments within Lisan Formation, but a similar or higher rate (an event per ~100 years) during the last millennium is indicated in Ze'elim Creek (Migowski et al. 2004). Agnon et al. (2006) argue that the resolution of seismites in the ~52 ka cluster of seismites in Lisan Formation at Peratzim Creek would not allow recording of a rate higher than an event in 200 year. Kagan et al. (2011) study seismites from the last two millennia in three sites currently onshore the Dead Sea northern basin. They distinguish events recorded simultaneously at the northernmost, the center, and the southernmost basin ("intra basin seismites" of Kagan et al. 2011). These events, seemingly with higher local intensity around the Dead Sea, show an average recurrence interval of ~200 years, about twice that of any individual section.

Marco et al. (1996) have used the *aperiodicity* (Eq. 8.4) to illustrate and quantify earthquake clustering in the distribution of intervals: if the aperiodicity is smaller than unity the distribution is periodic, whereas exceeding unity indicates clustering. The dated section of Lisan Formation has featured aperiodicity around 1.75. Agnon et al. (2006) found that the correction of the age model to include Haase-Schramm et al. (2004) dates decreases the aperiodicity only slightly to about 1.6.

Independent indication for long-term clustering has been reported for the Arava/Araba Valley (Fig. 8.1). Amit et al. (2002) dug paleoseismic trenches and dated clastic sediments with optically simulated luminescence (OSL) up to 90 ka. The dates constrained the ages of dip-slip events on marginal faults, showing more frequent activity of smaller events during the Holocene, and migration of activity across a shear zone.

The Holocene Dead Sea archive shows a quasi-periodic behavior. Aperiodicity for Ein Gedi core varied from 0.75 for the historic period to 0.9 for the entire upper 5 m (3.8 ka to present). The changes of recurrence during the late Quaternary may indicate transitions, or mode switchings, from clustered distributions via quasi-periodic distribution to a pronounced periodicity during the late Holocene. Such mode-switching was anticipated in simulations using two different physical models (Ben-Zion et al. 1999). Lyakhovsky et al. (1997) matched the behavior of the Lisan archive reported by Marco et al. (1996) with a model that explicitly computes distributed damage in the plate. In that model, mode-switching emerges when the rate of healing of fractures in the seismogenic zone balances the rate of mechanical loading (determined by the long-term slip rate). A simpler model that displays clustered versus periodic behavior accounts for distributed damage by stress variations off-fault (Kenner and Simons 2005).

Kagan et al (2005) found a mean recurrence interval of 10–14 kyear with aperiodicity of 0.6 for the cave seismites (interpreted to represent $M \geq 7.8$) during the last 185 kyear. These are likely of the largest events along the adjacent segment of DSR. However, correlation with lake seismites (discussed in the next section) does not show a consistent relationship with their clusters (Stein 2011), and in view of the completeness problem explained above, we may be looking at a partial set of such events.

A key variable in any long term seismological analysis is the ratio between the durations of the seismic cycle and the available archive. Each segment of the plate boundary may show a cycle given simply by the interval between the largest events on that segment. However, segments may interact in a complex manner, particularly where the plate boundary is complex (Braun et al. 2011). Several cycles of individual segments may combine to show a cycle for the system. Such cyclic behavior may explain the long-term earthquake clustering apparent in Lake lisan's record (Marco et al. 1996; Lyakhovsky et al. 1997).

Migowski et al. (2004) noted another manifestation of complex cycles: alternating periods (several centuries each) of high versus low rates of seismicity recorded in the Dead Sea basin, correlating them to similar periods in the East Anatolian fault (EAF, Fig. 8.1), and out of phase with the North Anatolian fault (NAF) (Ambraseys 1971). Agnon et al. (2006) found that the increase in activity at NAF and decrease at EAF at around 500 CE is heralded by a decrease at DSR, with more complicated relations around 1000 CE. These correlations suffer from two aspects: (1) the Anatolian data is somewhat out of date; (2) the Dead Sea record is local, biased due to minor events with epicenter close to the Dead Sea. In addition, a comparison of the rate of seismic moment release is likely to be more meaningful.

The recent compilation of the Dead Sea archive of historic seismites (Kagan et al. 2011) shows a cyclic behavior similar to the Ein Gedi core archive of Migowski et al. (2004) and Agnon et al. (2006) (Fig. 8.17a): the mean recurrence rate more than doubles during the tenth–twelfth centuries CE relative to the rest of the first millennium and the rest of the second millennium. The aperiodicity α calculated for that time (Eq. 8.4) changes only slightly around 0.6. Ambraseys (2006a, b, 2009) estimated magnitudes of 139 events during the period 100–2000 CE from macroseismic data and computed an average slip rate. He found an abrupt increase in slip rate after 1150 CE, from values that fluctuated between 0.22 and 0.26 cm/year since the 700 CE to the range 0.35–0.4 cm/year (Fig. 8.17b). Note that each of the three periods delineated in Fig. 8.17a is punctuated by a short interval of accelerated macro-seismic slip rate (Fig. 8.17b), associated with very large earthquakes. During the first period, this interval spans 530–560 CE, where the 551 CE earthquake (perhaps with associated activity) is recorded in the Dead Sea. The second period is associated with the 1156–1157 and 1170 CE earthquakes by Ambraseys' data (2006a, b, 2009). The third period is associated with the 1759 CE double event (Ambraseys and Barazangi 1989; Ellenblum et al. 1998). If this pattern is verifiable, it might have far reaching implications for the seismic behavior of the Dead Sea rift and other plate boundaries. However, a recent revised estimate of the 1170 and 1202 magnitudes (Hough and Avni 2011) might increase the acceleration of slip during this period (Table 8.3); more significantly, the revision would delay the timing of acceleration to the end of the middle period (thirteenth century). Figure 8.17 underscores the need for more paleoseismic data and additional historic macroseismic analyses.

Migowski et al. (2004) noted alternating activity cycles between south and north within DSR (see their Fig. 8.7b). Ambraseys (2006b, 2009) elaborated on this pattern (Ambraseys 2006b's Fig. 8.7). He inferred that earthquakes with $Ms \geq 7.2$

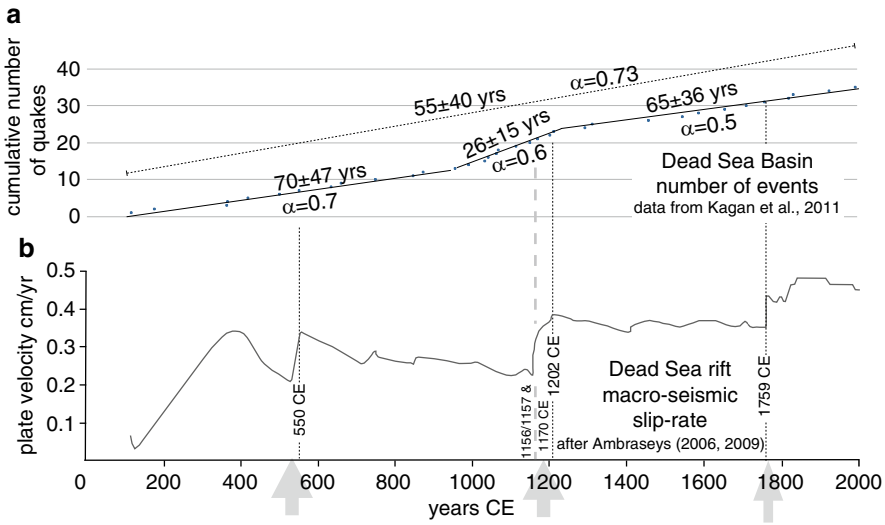

Fig. 8.17 Temporal variation of activity along the Dead Sea rift during the last nineteenth centuries. (**a**) cumulative number of events recorded by Dead Sea seismites (Fig. 8.13a; Kagan et al. 2011). The *slopes* of the graph suggest three periods with alternating recurrence intervals: 100–950 CE (70 ± 47 years), 950–1250 (26 ± 15 years), 1250–2000 (65 ± 36 years). The aperiodicities of the three periods are, respectively, 0.68, 0.57, and 0.55. For comparison, the mean recurrence interval for the entire period is 55 ± 40 years, with aperiodicity of 0.73. (**b**) Temporal variation of macro-seismic slip rate along the Dead Sea rift following the estimate by Ambraseys (2006a, b, 2009). Three periods of accelerated seismicity are discernible (*vertical gray arrows* beneath time axis), associated with the seismic episodes of the sixth-, twelfth-thirteenth-, and eighteenth-centuries CE (*vertical broken lines* denote historic earthquakes)

Table 8.3 Magnitude estimates of key historic earthquakes along the Dead Sea rift

Year CE	Ambraseys (2006b, 2009)	Other estimates	Reference
363	M 7.4	M 6.5–7	Present study[a]
551	M 7.3	M 7.4–7.6	Elias et al. (2007)
1170	M 7.3	M 7.5	Hough and Avni (2011)
1202	M 7.2	M 7.8	Hough and Avni (2011)

[a] The magnitude estimate is based on respective rupture of the Carmel fault along 60 km and the Arava/Araba Valley segment along 100 km. This choice seems appropriate for generating the damage pattern recorded by Russell (1980) and extended to account for the damage in Aila (Thomas et al. 2007)

propagate along a regular oscillatory trend. In view of the paleoseismic evidence from the Dead Sea, the assignment of M7.4 to the first event in the series (19 May 363 CE) is likely exaggerated – a result of amalgamation of the two events, one in the northern and the other in southern Holy Land. The revision of magnitudes of the 1170 and 1202 CE events (Hough and Avni 2011) further obliterates the oscillatory pattern inferred by Ambraseys (2006b, 2009).

Daeron et al. (2007) found a recurrence interval of 1.0–1.26 millennia for M ~ 7.5 ruptures on the Yammounneh fault, determined reliably for a limited period (~12–6.4 ka). Nemer et al. (2008) obtained similar results for the last six millennia. The dating uncertainty in both studies does not allow us to assess the aperiodicity.

Ferry et al. (2011) combined trenching, archaeology, and historical catalogues to study the earthquake history of the Jordan Valley (Fig. 8.1). They determined a mean recurrence interval of 790 years for the last four millennia, where intervals are smaller than age uncertainties. The standard deviation for this period is 520 years and the nominal aperiodicity at 0.66. This low figure is likely the result of the small number of intervals – (only five) and the limited period for which the dating precision is sufficient.

Ambraseys (2006b, 2009) compute frequency-size distributions for DSR. Notably, the macroseismic data covering the last two millennia are distributed significantly differently from the instrumental data. The macroseismic data taken together with the instrumental data seem to indicate a characteristic earthquake behavior with up to three times higher frequency for events of $M_s \geq 7$. Only if the assessment of M_s based on macroseismic analysis (Ambraseys 2006b, 2009) is systematically overestimated by the maximum reported uncertainty of 0.3, the distribution could follow a Gutenberg-Richter's relation. Yet if the macroseismic analysis has systematically underestimated the actual magnitudes, the Gutenberg-Richter relation underestimates the frequency of $M_s \sim 7$ by a factor around 30.

Hough and Avni (2011) construct a composite frequency-size distribution based on a modified version of the data of Ambraseys (2006b, 2009). The distribution, within the uncertainty of data, conform separate Gutenberg-Richter relations ("b-value" of unity) for either historical or instrumental data. For the M7, the historic earthquakes are four times more abundant than what would be predicted by extrapolation of the instrumental; for M7.6 the factor is 8. Ambraseys (2006b, 2009) frequency size relation for $4.5 \leq M_s \leq 5.5$ fits a Gutenberg-Richter relation with a similar "b value". The historical data then exceeds the extrapolation of instrumental data by a similar order, with a factor of about 5 between M_s6.7 and M_s7.3 .

To summarize the discussion of recurrence, the DSR shows variable recurrence in time and space (Table 8.2). The different types of archives with different sensitivities and uncertainties, and the bias of Dead Sea seismites toward local earthquakes, prevent definite statements to be made as yet. However, two broad conclusions can be drawn:

1. The historic period is represented well in the late Holocene lacustrine sections, with seemingly periodic behavior, with aperiodicity (standard deviation over mean recurrence interval) $\alpha \sim 0.6 \pm 0.1$. The common recurrence time is 65–70 years, yet between the tenth and the twelfth centuries CE the period is around 26 years.
2. While recurrence intervals for large earthquakes may be stable for periods up to several millennia, they are not stable over the 10-millennia duration scale. Yet, the longest archive of the strongest events, namely the speleoseismic archive, exhibits quasi-periodic behavior.

The latter conclusion may be a consequence of the incompleteness of this record, which is being complemented by further dating of damaged cave deposits. Alternatively, the largest earthquakes (say $M > 7.5$) may be controlled by the broad-scale segmentation of the rift, which may be considered constant for the 10–100 millennial time scale. Lyakhovsky et al. (1997) and by Kenner and Simons (2005) have proposed mechanical models for transitions between two patterns of frequency-size statistics and for the anoalous incidence of larger earthquakes. The large scale segmentation of the rift with segment lengths of ~100 km (Fig. 8.4b) may be reflected in the high abundance of larger earthquakes.

Acknowledgments The author is grateful to G.C.P. King and S. Wesnousky for thoughtful reviews, and to his numerous collaborators for inspiring discussions over two decades of research. Special thanks to E.J. Kagan for a meticulous editorial work. This research was supported by Israel Science Foundation (grant no. 1181/12), The German-Israeli Bi-national Science Foundation (GIF), the Helmholtz Association (Virtual Institute DESERVE), and by the Earth Science Administration in the Ministry of Energy and Water.

References

Adams J (1990) Paleoseismology of the Cascadia subduction zone – Evidence from turbidites off the Oregon-Washington margin. Tectonics 9:569–683. doi:10.1029/TC009i004p00569

Agnon A, Migowski C, Marco S (2006) Intraclast breccia layers in laminated sequences: recorders of paleo-earthquakes. Geol Soc Am Spec Pap 401:195–214

Akyuz HS, Altunel E, Karabacak V, Yalciner CC (2006) Historical earthquake activity of the northern part of the Dead Sea Fault Zone, southern Turkey. Tectonophysics 426:281–293. doi:10.1016/j.tecto.2006.08.005

Almagor G, Garfunkel Z (1979) Submarine slumping in continental margin and northern Sinai. Am Assoc Pet Geol Bull 63:324–340

Alsop GI, Marco S (2011) Soft-sediment deformation within seismogenic slumps of the Dead Sea Basin. J Struct Geol 33:433–457. doi:10.1016/j.jsg.2011.02.003

Al-Qaryouti MY (2008) Attenuation relations of peak ground acceleration and velocity in the Southern Dead Sea Transform region. Arab J Geosci 1:111–117. doi:10.1007/s12517-008-0010-4

Ambraseys NN (1971) Value of historical records of earthquakes. Nature 232:375–379

Ambraseys NN (1998) The earthquake of 1 January 1837 in southern Lebanon and northern Israel. Ann Geophys 15:923–935

Ambraseys NN (2005a) The seismic activity in Syria and Palestine during the middle of the 8th century; an amalgamation of historical earthquakes. J Seismol 9:115–125

Ambraseys N (2005b) Historical earthquakes in Jerusalem – A methodological discussion. J Seismol 9:329–340

Ambraseys N (2006a) Earthquakes and archaeology. J Archaeol Sci 33:1008–1016. doi:10.1016/j.jas.2005.11.006

Ambraseys NN (2006b) Comparison of frequency of occurrence of earthquakes with slip rates from long-term seismicity data: the cases of Gulf of Corinth, Sea of Marmara and Dead Sea Fault Zone. Geophys J Int 165:516–526. doi:10.1111/j.1365-246X.2006.02858.x

Ambraseys NN (2009) Earthquakes in the Mediterranean and Middle East: a multidisciplinary study of seismicity up to 1900. Cambridge University Press, New York, 947 pp

Ambraseys NN, Barazangi M (1989) The 1759 earthquake in the Bekaa valley. Implications for earthquake hazard assessment in the eastern Mediterranean region. J Geophys Res 94:4007–4013

Ambraseys NN, Jackson JA (1998) Faulting associated with historical and recent earthquakes in the Eastern Mediterranean region. Geophys J Int 133:390–406

Ambraseys N, Karcz I (1992) The earthquake of 1546 in the Holy Land. Terra Nova 4:253–262. doi:10.1111/j.1365-3121.1992.tb00480.x

Ambraseys NN, Melville CP (1988) An analysis of the eastern Mediterranean earthquake of 20 May 1202. In: Lee WKH et al (eds) History of seismography and earthquakes of the world. Academic, San Diego, pp 181–200

Ambraseys N, Synolakis C (2010) Tsunami catalogs for the Eastern Mediterranean revisited. J Earthq Engin 14:309–330. doi:10.1080/13632460903277593

Ambraseys NN, Melville CP, Adams RD (1994) The seismicity of Egypt, Arabia and the Red Sea: a historical review. Cambridge University Press, New York, 181 pp. doi:10.1017/CBO9780511524912

Amiran D, Arieh E, Turcotte T (1994) Earthquakes in Israel and adjacent areas: macroseismic observations since 100 BCE. Isr Expl J 44:260–305. (Correction, Isr Explor J 45: 201, 1995)

Amit R, Zilberman E, Enzel Y, Porat N (2002) Paleoseismic evidence for time dependency of seismic response on a fault system in the southern Arava Valley, Dead Sea rift, Israel. Geol Soc Am Bull 114:192–206

Amitai R (1989) Notes on the Ayyūbid Inscriptions at al-Ṣubayba (Qalʿat Nimrūd). Dumbart Oaks Pap 43:113–119

Atkinson GM, Wald DJ (2007) "Did you feel it"? Intensity data: a surprisingly good measure of earthquake ground motion. Seismol Res Lett 78:362–368. doi:10.1785/gssrl.78.3.362

Austin SA, Franz GW, Frost EG (2000) Amos's earthquake: an extraordinary Middle East seismic event of 750 BC. Int Geol Rev 42:657–671

Avner U (1998) Settlement, agriculture and paleoclimate in Uvda Valley, southern Negev desert, 6th-3rd millenia BC. In: Issar AS, Brown N (eds) Water, environment and society in times of climatic change. Kluwer Academic Publishers, Dordrecht, pp 147–202

Avner U, Carmi I, Segal D (1994) Neoloithic to Bronze Age settlmentof the Negev and Sinai in light of radio- carbon dating. A view from the South- ern Negev. In: Bar-Yosef O, Kra RS (eds) Late Quaternary chronology and paleoclimates of the eastern Mediterranean. Radiocarbon, Tucson, pp 265–300

Avni R (1999) The 1927 Jericho earthquake: comprehensive Macro- seismic analysis based on contemporary sources. Ben-Gurion University of the Negev, Beersheba, 203 pp

Baer G, Funning GJ, Shamir G, Wright TJ (2008) The 1995 November 22, M(w) 7.2 Gulf of Elat earthquakecyclerevisited.GeophysJInt175:1040–1054.doi:10.1111/j.1365-246X.2008.03901.x

Bakun WH, Wentworth CM (1997) Estimating earthquake location and magnitude from seismic intensity data. Bull Seismol Soc Am 87:1502–1521

Bar-Matthews M, Ayalon A, Kaufman A (2000) Timing and hydrological conditions of sapropel events in the Eastern Mediterranean, as evident from speleothems, Soreq Cave, Israel. Chem Geol 169:145–156

Barkan E, Luz B, Lazar B (2001) Dynamics of the carbon dioxide system in the Dead Sea. Geochem Cosmochem Acta 65:355–368

Bartov Y, Stein M, Enzel Y, Agnon A, Reches Z (2002) Lake levels and sequence stratigraphy of Lake Lisan, the late Pleistocene precursor of the Dead Sea. Quat Res 57:9–21. doi:10.1006/qres.2001.2284

Begin ZB, Ehrlich A, Nathan Y (1974) Lake Lisan, the Pleistocene precursor of the dead sea. Geol Surv Isr Bull 63:30pp

Belmaker R, Stein M, Yechieli Y, Lazar B (2007) Controls on the radiocarbon reservoir ages in the modern Dead Sea drainage system and in the last glacial Lake Lisan. Radiocarbon 49:969–982

Ben-Menahem A (1979) Earthquake catalogue for the Middle East (92 B.C. to 1980 A.D.). Boll Geofis Teor Appl 21:245–313

Ben-Menahem A (1991) Four thousand years of seismicity along the Dead Sea rift. J Geophys Res 96:20195–20216
Ben-Zion Y, Damen K, Lyakhovsky V, Ertas D, Agnon A (1999) Spontaneous mode switching of earthquakes, Earth Planet. Sci Lett 172:11–21
Bikai PM (2002) The churches of Byzantine Petra, in Petra: a Royal City unearthed. Near East Archaeol 65:271–276
Bookman R, Enzel Y, Agnon A, Stein M (2004) Late Holocene lake levels of the Dead Sea. Geol Soc Am Bull 116:555–571
Bourke SJ (2004) Cult and archaeology at Pella in Jordan: excavating the Bronze and Iron Age temple precinct (1994–2001). J Proc R Soc N S W 137:1–31
Bourke S, Sparks R, Mairs L (1999) Bronze age occupation on Tell Husn (Pella): report on the University of Sydney's 1994/95 field seasons. Mediterr Archaeol 12:51–66
Bowman D (1971) Geomorphology of the shore terraces of the late Pleistocene Lisan Lake (Israel). Palaeogeogr palaeoclim Palaeoecol 9:183–209. doi:10.1016/0031-0182(71)90031-9
Braun Y (2009) Dating paleo-seismic activity on the Carmel fault using damaged cave deposits from Denya Cave, Mt. Carmel. M.Sc. thesis, The Hebrew University of Jerusalem, Jerusalem, 87 pp
Braun Y, Kagan E, Bar-Matthews M, Ayalon A, Agnon A (2011) Dating speleoseismites near the Dead Sea Transform and the Carmel fault: clues to coupling of a plate boundary and its branch. Isr J Earth Sci 58:257–273. doi:10.1560/IJES.58.3-4.257. Spec. vol., eds. Agnon A, Amit R, Michetti A, Hough S, The Dead Sea rift as a natural laboratory for neotectonics and paleoseismology
Chapron E, Beck C, Pourchet M, Deconinck JF (1999) 1822 earthquake-triggered homogenite in Lake Le Bourget (NW Alps). Terra Nova 11:86–92. doi:10.1046/j.1365-3121.1999.00230.x
Cita MB, Beghi C, Camerlenghi A, Kastens KA, McCoy FW, Nosetto A, Parisi E, Scolari F, Tomadin L (1984) Turbidites and megaturbidites from Herodotus Abyssal-Plain (Eastern Mediterranean) unrelated to seismic events. Mar Geol 55:79–101. doi:10.1016/0025-3227(84)90134-8
Cita MB, Camerlenghi A, Rimoldi B (1996) Deep-sea tsunami deposits in the eastern Mediterranean: new evidence and depositional models. Sediment Geol 104(1–4):155–173. doi:10.1016/0037-0738(95)00126-3
Davenport CA, Ringrose PS (1987) Deformation of Scottish Quaternary sediment sequence by strong earthquake motions. In: Jones ME, Preston RM (eds) Deformation of sediments and sedimentary rocks, Geological Society special publication, 29. Geological Society by Blackwell Scientific, Oxford/London, pp 299–314
Daeron M, Klinger Y, Tapponnier P, Elias A, Jacques E, Sursock A (2007) 12,000-year-long record of 10 to 13 Paleoearthquakes on the Yammoûneh Fault, Levant Fault System, Lebanon. Bull Seismol Soc Am 97:749–771. doi:10.1785/0120060106
Deves M, King GCP, Klinger Y, Agnon A (2011) Localised and distributed deformation in the lithosphere: modelling the Dead Sea region in 3 dimensions. Earth Planet Sci Lett 308:172–184. doi:10.1016/j.epsl.2011.05.044
Doig R (1990) 2300 yr history of seismicity from silting events in Lake Tadoussac, Charlevoix, Quebec. Geology 18:820–823
Doig R (1991) Effects of strong seismic shaking in lake sediments, and earthquake recurrence interval, Témiscaming, Quebec. Can J Earth Sci 28:1349–1352
Doig R (1998) 3000-year paleoseismological record from the region of the 1988 Saguenay, Quebec, earthquake. Bull Seismol Soc Am 88:1198–1203
Eklund S (2008) Stone weathering in the monastic building complex on Mountain of St Aaron in Petra, Jordan. M.A. thesis, University of Helsinki Institute for Cultural Studies Department of Archaeology, 113 p
Elias A, Tapponnier P, Singh SC, King GCP, Briais A, Daeron M, Carton H, Sursock A, Jaques E, Jomaa R, Klinger Y (2007) Active thrusting offshore Mount Lebanon: source of the tsunamigenic A.D. 551 Beirut-Tripoli earthquake. Geology 35:755–758. doi:10.1130/G23631A.1

El-Isa ZH, Mustafa H (1986) Earthquake deformations in the Lisan deposits and seismotectonic implications. Geophys J R Astron Soc 86:413–424
Ellenblum R (1989) Who built Qalʿat al-Ṣubayba? Who built Qalʿat al-Ṣubayba? Dumbart Oaks Pap 43:103–112
Ellenblum R (2007) Crusader castles and modern histories. Cambridge University Press, Cambridge, 362 pages
Ellenblum R, Marco S, Agnon A, Rockwell T, Boas A (1998) A Crusader castle torn apart by the 1202 earthquake. Geology 26:303–306
Enzel Y, Kadan G, Eyal Y (2000) Holocene earthquakes inferred from a fan-delta sequence in the Dead Sea graben. Quat Res 53:34–48
Enzel Y, Agnon A, Stein M (eds) (2006) New frontiers in Dead Sea paleoenvironmental research, Geological Society of America special paper 401. Geological Society of America, Boulder
Fantalkin A, Finkelstein I (2006) The Sheshonq I campaign and the 8th-century BCE earthquake-more on the archaeology and history of the South in the Iron I-IIa. J Inst Archaeol Tel Aviv Univ 33:18–42
Ferry M, Meghraoui M, Abou Karaki NA, Al Taj M, Khalil L (2011) Episodic behavior of the Jordan Valley section of the Dead Sea fault inferred from a 14-ka-long integrated catalog of large earthquakes. Bull Seismol Soc Am 101:39–67. doi:10.1785/0120100097
Franken HJ (1992) Excavations at Tell Deir ʻAlla. The late bronze age sanctuary. Peeters, Louvain
Garfunkel Z (2011) The long- and short-term lateral slip and seismicity along the Dead Sea Transform: an interim evaluation. Isr J Earth Sci, Spec Vol, Agnon A, Amit R, Michetti A, Hough S (eds) The Dead Sea rift as a natural laboratory for neotectonics and paleoseismology (in press)
Garfunkel Z, Zak I, Freund R (1981) Active faulting in the Dead Sea rift. Tectonophysics 80:1–26
Gibert L, Alfaro P, Garcia-Tortosa FJ, Scott G (2011) Superposed deformed beds produced by single earthquakes (Tecopa Basin, California): insights into paleoseismology. Sediment Geol 235:148–159. doi:10.1016/j.sedgeo.2010.08.003
Gluck D (2001) The landscape evolution of the south western Dead Sea Basin and the paleoseismic record of the south western marginal fault of the Dead Sea Basin and of the Carmel fault during the Late Pleistocene and Holocene. M.Sc. thesis, Hebrew University, Jerusalem, Israel [in Hebrew with English abstract]
Goes SDB (1996) Irregular recurrence of large earthquakes: an analysis of historic and paleoseismic catalogs. J Geophys Res 101:5739–5749. doi:10.1029/95JB03044
Guidoboni E, Comastri A (2005) Catalogue of earthquakes and tsunamis in the Mediterranean Area from the 11th to the 15th Century. INGV-SGA, Bologna
Guidoboni E, Comastri A, Traina G (1994) Catalogue of ancient earthquakes in the Mediterranean area up to the 10th century. INGV-SGA, Rome
Haase-Schramm A, Goldstein SL, Stein M (2004) U–Th dating of Lake Lisan aragonite (Late Pleistocene Dead Sea) and implications for glacial East Mediterranean climate change. Geochim Cosmochim Acta 68:985–1005
Hall JK (1996) Digital topography and bathymetry of the area of the Dead Sea depression. Tectonophysics 266:177–185. doi:10.1016/S0040-1951(96)00189-8
Hammond PC (1980) New evidence for the 4th-century A. D. destruction of Petra. Bull Am Sch Orient Res 238:65–67
Hanfmann GMA (1951) The Bronze Age in the Near East: a review article [Part I]. Am J Archaeol 55:355–365
Hartal M (2001) The al-Subayba (Nimrod) fortress: towers 11 and 9. With contributions by Amitai R, Boas A. (Israel Antiquities Authority reports no. 11.) pp. 130, 197 line drawings and half-tones, 22 plans in text. Israel Antiquities Authority, Jerusalem
Haynes JM, Niemi TM, Atallah M (2006) Evidence for ground-rupturing earthquakes on the Northern Wadi Araba fault at the archaeological site of Qasr Tilah, Dead Sea Transform fault system, Jordan. J Seismol 10:415–430. doi:10.1007/s10950-006-9028-9
Heezen BC, Ewing M (1952) Turbidity currents and submarine slumps, and the 1929 Grand Banks [Newfoundland] earthquake. Am J Sci 250:849–873. doi:10.2475/ajs.250.12.849

Heifetz E, Agnon A, Marco S (2005) Soft sediment deformation by Kelvin-Helmholtz instability: a case from Dead Sea earthquakes. Earth Planet Sci Lett 236:497–504

Hempton MR, Dewey JF (1983) Earthquake-induced deformational structures in young lacustrine sediments, East Anatolian Fault, southern Turkey. Tectonophysics 98:T7–T14. doi:10.1016/0040-1951(83)90294-9

Hennessey IB (1969) Preliminary report on a first season of excavation sat Telleilat Ghassul. Levant 1:1–24

Herzog Z, Singer-Avitz L (2004) Redefining the centre: the emergence of State in Judah. J Inst Archaeol Tel Aviv Univ 31:209–244

Hinzen KG (2011) Sensitivity of earthquake toppled columns to small changes in ground motion and geometry. Isr J Earth Sci 58:309–326

Hough SE, Avni R (2011) The 1170 and 1202 CE Dead Sea Rift earthquakes and long-term magnitude distribution of the Dead Sea Fault zone. Isr J Earth Sci 58:295–308. doi:10.1560/IJES.58.3-4.295. Spec. Vol., eds. Agnon A, Amit R, Michetti A, Hough S, The Dead Sea rift as a natural laboratory for neotectonics and paleoseismology

Jones AP, Omoto K (2000) Towards establishing criteria for identifying trigger mechanisms for soft-sediment deformation: a case study of Late Pleistocene lacustrine sands and clays, Onikobe and Nakayamadaira Basins, northeastern Japan. Sedimentology 47:1211–1226

Kagan E (2011) Multi-archive paleoseismology along the southern Dead Sea rift: independent recording by lake and cave sediments. PhD thesis, Hebrew University, Jerusalem

Kagan E, Bar-Matthews M, Ayalon A, Agnon A (2005) Dating large and infrequent earthquakes using damaged cave deposits. Geology 33:251–264

Kagan EJ, Stein M, Agnon A, Bronk Ramsey C (2010) Paleoearthquakes as anchor points in Bayesian radiocarbon deposition models: a case study from the Dead Sea. Radiocarbon 54(3):1018–1026

Kagan E, Stein M, Agnon A, Neumann F (2011) Intrabasin paleoearthquake and quiescence correlation of the late Holocene Dead Sea. J Geophys Res 116:B04311. doi:10.1029/2010JB007452

Kastens KA (1984) Earthquakes as a triggering mechanism for debris flows and turbidites on the Calabrian ridge. Mar Geol 55:13–33. doi:10.1016/0025-3227(84)90130-0

Karcz Y (2004) Implications of some early Jewish sources for estimates of earthquake hazard in the Holy Land. Ann Geophys 47:759–792

Karcz Y, Kafri U (1978) Evaluation of supposed archaeoseismic damage in Israel. J Archaeol Sci 5:237–253

Karcz I, Kafri U, Meshel Z (1977) Archaeological evidence for subrecent seismic activity along the Dead Sea–Jordan rift. Nature 269:234–235

Katz O, Crouvi O (2007) The geotechnical effects of long human habitation (2000 < years): earthquake induced landslide hazard in the city of Zefat, northern Israel. Eng Geol 95:57–78

Katz A, Kolodny Y, Nissenbaum A (1977) The geochemical evolution of the Pleistocene Lake Lisan–Dead Sea system. Geochim Cosmochim Acta 41:1609–1626. doi:10.1016/0016-7037(77)90172-7

Katz A, Agnon A, Marco S (2009) Earthquake-induced barium anomalies in the Lisan Formation, Dead Sea rift valley. Isr Earth Planet Sci Lett 286:219–229. doi:10.1016/j.epsl.2009.06.031

Katz O, Amit R, Yagoda-Biran G, Hatzor YH, Porat N, Medvedev B (2011) Quaternary earthquakes and landslides in the Sea of Galilee area, the Dead Sea Transform: paleoseismic analysis and implication to the current hazard. Isr J Earth Sci 58:275–294. doi:10.1560/IJES.58.3-4.275. Spec. vol, eds. Agnon A, Amit R, Michetti A, Hough S, The Dead Sea rift as a natural laboratory for neotectonics and paleoseismology

Kenner SJ, Simons M (2005) Temporal clustering of major earthquakes along individual faults due to post-seismic reloading. Geophys J Int 160:179–194. doi:10.1111/j.1365-246X.2005.02460.x

Ken-Tor R, Agnon A, Enzel Y, Marco S, Negendank JFW, Stein M (2001) High resolution geological record of historic earthquakes in the Dead Sea Basin. J Geophys Res 106:2221–2234

Kesten D, Weber M, Haberland C, Janssen C, Agnon A, Bartov Y, Rabba I, The DESERT Group (2008) Combining satellite and seismic images to analyse the shallow structure of the Dead Sea Transform near the DESERT transect. Int J Earth Sci (Geol Rundsch). doi:10.1007/s00531-006-0168-5

Klinger Y, Rivera L, Haessler H, Maurin JC (1999) Active faulting in the Gulf of Aqaba: new knowledge from the M-W 7.3 earthquake of 22 November 1995. Bull Seismol Soc Am 89:1025–1036

Klinger Y, Avouac JP, Dorbath L, Abou Karaki N, Tisnerat N (2000) Seismic behaviour of the Dead Sea fault along Araba valley, Jordan. Geophys J Int 142:769–782. doi:10.1046/j.1365-246x.2000.00166.x

Levi TE, Adams RB, Hauptmann A, Prange M, Schmitt-Schtrecker S, Najjar M (2002) Early Bronze Age metallurgy: a newly discovered copper manufactory in southern Jordan. Antiquity 76:425

Levi T, Weinberger R, Aifa T, Eyal Y, Marco S (2006) Earthquake-induced clastic dikes detected by anisotropy of magnetic susceptibility. Geology 3:69–72. doi:10.1130/G22001.1

Lyakhovsky V, Ben-Zion Y, Agnon A (1997) Distributed damage, faulting, and friction. J Geophys Res 102:27635–27649

Lioubashevski O, Hamiel Y, Agnon A, Reches Z, Fineberg J (1999) Oscillons and solitary waves in a vertically vibrated colloidal suspension. Phys Rev Lett 83:3190–3193

Magness J (1997) Synagogue typology and earthquake chronology at Khirbet Shema', Israel. J Field Archaeol 24:211–220

Makdisi G (1956) Autograph Diary of an Eleventh-Century Historian of Baghdad. Bull Sch Orient Afr Stud 1:9–31

Machlus M, Enzel Y, Goldstein SL, Marco S, Stein M (2000) Reconstruction of low-stands of Lake Lisan between 55 and 35 kyr. Quat Int 73–74:137–144. doi:10.1016/S1040-6182(00)00070-7

Makovsky Y, Wunch A, Ariely R, Shaked Y, Rivlin A, Shemesh A, Ben-Avraham Z, Agnon A (2008) Quaternary transform kinematics constrained by sequence stratigraphy and submerged coastline features: the Gulf of Aqaba. Earth Planet Sci Lett 271:109–122

Malkawi AIH, Fahmi KJ (1996) Locally derived earthquake ground motion attenuation relations for Jordan and conterminous areas. Q J Eng Geol Hydrogeol 29:309–319. doi:10.1144/GSL.QJEGH.1996.029.P4.05

Manspeizer W (1985) The Dead Sea rift: impact of climate and tectonism on Pleistocene and Holocene sediments. In: Biddle KT, Christie-Black N (eds) Strike-slip deformation, basin formation and sedimentation, Society for Economic Paleontology and Mineralogy special publication 37. The Society, Tusla, pp 143–158

Marco S (2008) Recognition of earthquake-related damage in archaeological sites: examples from the Dead Sea fault zone. Tectonophysics 453:148–156. doi:10.1016/j.tecto.2007.04.011

Marco S, Agnon A (1995) Prehistoric earthquake deformations near Massada, the Dead Sea graben. Geology 23:695–698

Marco S, Agnon A (2005) Repeated earthquake faulting revealed by high-resolution stratigraphy. Tectonophysics 408:101–112

Marco S, Agnon A, Ellenblum R, Eidelman A, Basson U, Boaz A (1997) 817-year-old walls offset sinistrally 2.1 m by the Dead Sea Transform, Israel. J Geodyn 24:11–20

Marco S, Agnon A, Finkelstein I, Ussishkin D (2006) Ch. 31: Megiddo earthquakes. In: Megiddo IV. E. and C. Yass Publications in Archaeology, Tel-Aviv, pp 569–575

Marco S, Klinger Y (2014) Review of on-fault Palaeo-seismic studies along the Dead Sea Fault. In: Garfunkel Z et al (eds) Dead Sea transform fault system: reviews, Modern approaches in solid earth sciences 6. Springer, Dordrecht

Marco S, Hartal M, Hazan N, Lev L, Stein M (2003) Archaeology, history, and geology of the A.D. 749 earthquake, Dead Sea transform. Geology 31:665–668. doi:10.1130/G19516.1

Marco S, Rockwell T, Agnon A, Heimann A, Frieslander U (2005) Late Holocene slip of the Dead Sea Transform revealed in 3D palaeoseismic trenches on the Jordan Gorge Fault. Earth Planet Sci Lett 234:189–205

Marco S, Stein M, Agnon A, Ron H (1996) Long term earthquake clustering: a 50,000 year paleoseismic record in the Dead Sea Graben. J Geophys Res 101:6179–6192

Marco S, Weinberger R, Agnon A (2002) Radial clastic dykes formed by a salt diapir in the Dead Sea Rift, Israel. Terra Nova 14:288–294

Matmon A, Shaked Y, Agnon A, Porat N, Enzel Y, Finkel R, Lifton N, Boarretto E (2005) Lessons to exposure age dating from constraining the time of earthquake induced rockfalls along the margins of the Dead Sea fault system, southern Israel. Earth Planet Sci Lett 240:803–817

McCalpin JP (ed) (2009) Paleoseismology, 2nd edn. Academic, San Diego

McHugh CMG, Seeber L, Cormier M-H, Dutton J, Cagatay N, Polonia A, Ryan WBF, Gorur N (2006) Submarine earthquake geology along the North Anatolia Fault in the Marmara Sea. Earth Planet Sci Lett 248:661–684. doi:10.1016/j.epsl.2006.05.038

Meghraoui M, Gomez F, Sbeinati R, Van der Woerd J, Mouty M, Darkal AN, Radwan Y, Layyous I, Al Najjar H, Darawcheh R, Hijazi F, Al-Ghazzi R, Barazangi M (2003) Evidence for 830 years of seismic quiescence from palaeoseismology, archaeoseismology and historical seismicity along the Dead Sea fault in Syria. Earth Planet Sci Lett 210:35–52. doi:10.1016/S0012-821X(03)00144-4

Meyers EM, Kraabel AT, Strange JF (1976) Ancient synagogue excavations at Khirbet Shema', Upper Galilee, Israel, 1970–1972, Ann Amer Sch Orient Res XLII. Duke University Press, Durham

Migowski C, Agnon A, Bookman R, Negendank JFW, Stein M (2004) Recurrence pattern of Holocene earthquakes along the Dead Sea transform revealed by varve-counting and radiocarbon dating of lacustrine sediments. Earth Planet Sci Lett 222:301–314

Monecke K, Anselmetti FS, Becker A, Schnellmann M, Sturm M, Giardini D (2006) Earthquake-induced deformation structures in lake deposits: a late Pleistocene to holocene paleoseismic record for central Switzerland. Ecol Geol Helv 99:343–362. doi:10.1007/s00015-006-1193-x

Moretti M, Alfaro P, Caselles O et al (1999) Modelling seismites with a digital shaking table. Tectonophysics 304:369–383

Moretti M, Sabato L (2007) Recognition of trigger mechanisms for soft-sediment deformation in the Pleistocene lacustrine deposits of the Sant'Arcangelo Basin (Southern Italy): seismic shock vs. overloading. Sediment Geol 196:31–45. doi:10.1016/j.sedgeo.2006.05.012

Morhange C, Pirazzoli PA, Marriner N, Montagioni LF, Nanmour T (2006) Late Holocene relative sea-level changes in Lebanon, East- ern Mediterranean. Mar Geol 230:99–114. doi:10.1016/j.margeo.2006.04.003

Nemer T, Gomez F, Al Haddad S, Tabet C (2008) Coseismic growth of sedimentary basins along the Yammouneh strike-slip fault (Lebanon). Geophys J Int 175:1023–1039

Neumann FHS, Kagan EJS, Stein MPI, Agnon API (2009) Assessment of the effect of earthquake activity on regional vegetation – High-resolution pollen study of the Ein Feshka section, Holocene Dead Sea. Rev Palaeobot Palynol 155:42–51

Nur A (2008) Apocalypse: earthquakes, archaeology, and the wrath of God. Princeton University Press, Princeton. ISBN 9780691016023

Nur A, Cline EH (2000) Poseidon's horses: plate tectonics and earthquake storms in the LateBronze Age Aegean and Eastern Mediterranean. J Archaeol Sci 27:43–63

Oth A, Wenzel F, Wust-Bloch H, Gotschammer E, Ben-Avraham Z (2007) Parameterization of a composite attenuation relation for the Dead Sea area based on 3-D modeling of elastic wave propagation. Pure Appl Geophys 164:23–37. doi:10.1007/s00024-006-0147-6

Owen G, Moretti M, Alfaro P (2011) Recognising triggers for soft-sediment deformation: current understanding and future directions. Sediment Geol 235:133–140

Pettijohn FJ, Potter PE (1964) Atlas and glossary of primary sedimentary structures. Springer-Verlag, Berlin, Science – 370pp

Porat N, Levi T, Weinberger R (2007) Possible resetting of quartz OSL signals during earthquakes-evidence from late Pleistocene injection dikes, Dead Sea basin. Isr Quat Geochronol 2:272–277. doi:10.1016/j.quageo.2006.05.021

Porat N, Duller GAT, Roberts HM, Piasetzky E, Finkelstein I (2012) OSL dating in multi-strata Tel: Megiddo (Israel) as a case study. Quat Geochronol 10:359–366. doi:10.1016/j.quageo.2011.11.011

Prasad S, Negendank JFW, Stein M (2009) Varve counting reveals high resolution radiocarbon reservoir age variations in palaeolake Lisan. J Quat Sci 24:690–696
Reinhardt EG, Goodman BN, Boyce JI, Lopez G, van Hengstum P, Rink WJ, Mart Y, Raban A (2006) The tsunami of 13 December A.D. 115 and the destruction of Herod the Great's harbor at Caesarea Maritima, Israel. Geology 34:1061–1064. doi:10.1130/G22780A.1
Roep TB, Everts AJ (1991) Pillow-beds – A new type of seismites – An example from an Oligocene turbidite fan complex, Alicante, Spain. Sedimentology 39:711–724. doi:10.1111/j.1365-3091.1992.tb02148.x
Ron H, Nowaczyk NR, Frank U, Schwab MJ, Naumann R, Striewski B, Agnon A (2007) Greigite detected as dominating remanence carrier in Late Pleistocene sediments, Lisan formation, from Lake Kinneret (Sea of Galilee), Israel. Geophys J Int 170:117–131. doi:10.1111/j.1365-246X.2007.03425.x
Rucker JD, Niemi TM (2010) Historical earthquake catalogues and archaeological data: achieving synthesis without circular reasoning. In: Sintubin M, Stewart IS, Niemi TM, Altunel E (eds) Ancient earthquakes, Geological Society of America special paper 471. Geological Society of America, Boulder, pp 97–106
Russell K (1980) The earthquake of May 19, A.D. 363. Bull Am Sch Orient Res 238:47–63
Salamon A (2010) Patterns of seismic sequences in the Levant – Interpretation of historical seismicity. J Seismol 14:339–367. doi:10.1007/s10950-009-9168-9
Salamon A, Rockwell T, Guidoboni E, Comastri E (2011) A critical evaluation of tsunami records reported for the Levant Coast from the second millennium BCE to the present. Isr J Earth Sci 58:327–354. doi:10.1560/IJES.58.2-3.327
Salamon A, Rockwell T, Ward SN, Guidoboni E, Comastri A (2007) Tsunami hazard evaluation of the eastern Mediterranean: historical analysis and selected modeling. Bull Seismol Soc Am 97:705–724
Sbeinati MR, Darawcheh R, Mouty M (2005) The historical earthquakes of Syria: an analysis of large and moderate earthquakes from 1365 B.C. to 1900 A.D. Ann Geophys 48:347–435
Sbeinati MR, Meghraoui M, Suleyman G, Gomez F, Grootes P, Nadeau MJ, Al Najjar H, Al Ghazzi R (2010) Timing of earthquake ruptures at the Al Harif Roman aqueduct (Dead Sea fault, Syria) from archaeoseismology and paleoseismology. In: Sintubin M, Stewart IS, Niemi TM, Altunel E (eds) Ancient earthquakes, Geological Society of America special paper 471. Geological Society of America, Boulder, pp 244–267
Schaeffer CFA (1948) Stratigraphic Compareé et Chronologie de l'Asie Occidental. Oxford University Press, New York, 653 pp
Seilacher A (1969) Fault-graded beds interpreted as seismites. Sedimentology 13:155–159
Seilacher A (1984) Sedimentary structures tentatively attributed to seismic events. Mar Geol 55:1–12
Segal A (2007) The Churches of Sussita, Interim Report at the End of Seven Excavation Seasons (2000–2006). http://hippos.haifa.ac.il/index.php/8-general/36-churches-hippos
Shaked Y, Agnon A, Lazar B, Marco S, Avner U, Stein M (2004) Large earthquakes kill coral reefs at the north-west Gulf of Aqaba. Terra Nova 16:133–138
Shaked Y, Lazar B, Marco S, Stein M, Agnon A (2011) Late Holocene events that shaped the shoreline at the northern Gulf of Aqaba as recorded by a buried reef. Isr J Earth Sci 58. Spec. vol, eds. Agnon A, Amit R, Michetti A, Hough S, The Dead Sea rift as a natural laboratory for neotectonics and paleoseismology (in press)
Shamir G, Baer G, Hofstetter A (2003) Three-dimensional elastic earthquake modelling based on integrated seismological and InSAR data: the M-w = 7.2 Nuweiba earthquake, gulf of Elat/Aqaba 1995 November. Geophys J Int 154:731–744. doi:10.1046/j.1365-246X.2003.01978.x
Shaw SW (1947) Southern Palestine: geological map on a scale of 1:250,000 with explanatory notes. Govt. Printer, Jerusalem, 42 pp
Siegenthaler C, Finger W, Kelts K, Wang S (1987) Earthquake and seiche deposits in Lake Lucerne, Switzerland. Eclogae Geol Helv 80:241–260
Sieh K (1978) Prehistoric large earthquakes produced by slip on the San Andreas fault at Pallett Creek, California. J Geophys Res 83:3907–3939. doi:10.1029/JB083iB08p03907

Sims JD (1973) Earthquake-induced structures in sediments of sediments of Van Norman Lake, San Fernando, California. Science 182:161–163
Sims JD (1975) Determining earthquake recurrence intervals from deformational structures in young lacustrine sediments. Tectonophysics 29:153–159
Slater L, Niemi TM (2003) Detection of active faults along the Dead Sea Transform using ground penetrating radar and implications for seismic hazards within the city of Aqaba, Jordan. Tectonophysics 368:33–50
Stein M (2011) Paleo-earthquakes chronometry in the late Quaternary Dead Sea basin. Isr J Earth Sci 58:237–255. doi:10.1560/IJES.58.3-4.237. Spec. vol, eds. Agnon A, Amit R, Michetti A, Hough S, The Dead Sea rift as a natural laboratory for neotectonics and paleoseismology
Stiros SC (2001) The AD 365 Crete earthquake and possible seismic clustering during the fourth to sixth centuries AD in the Eastern Mediterranean: a review of historical and archaeological data. J Struct Geol 23:545–562. doi:10.1016/S0191-8141(00)00118-8
Swan FH, Schwartz DP, Cluff LS (1980) Recurrence of moderate to large magnitude earthquakes produced by surface faulting on the Wasatch fault zone, Utah. Bull Seismol Soc Am 70:1431–1462
Thacker WC, Lavelle JW (1977) Two-phase flow analysis of hindered settling. Phys Fluids 20:1577–1579
Thomas R, Parker ST, Niemi TM (2007) Structural damage from earthquakes in the second-ninth centuries at the archaeological site of Aila in Aqaba, Jordan. Bull Am Sch Orient Res 346:59–77
Tibor G, Niemi TM, Ben-Avraham Z, Al-Zoubi A, Sade RA, Hall JK, Hartman G, Akawi E, Abueladas A, Al-Ruzouq R (2010) Active tectonic morphology and submarine deformation of the northern Gulf of Eilat/Aqaba from analyses of multibeam data. Geomarine Lett 30:561–573. doi:10.1007/s00367-010-0194-y
Torfstein A, Gavrieli I, Katz A et al (2008) Gypsum as a monitor of the paleo-limnologicalhydrological conditions in Lake Lisan and the Dead Sea. Geochimica Cosmochimica Acta 72:2491–2509
Tsafrir Y, Foerster G (1997) Urbanism at Scythopolis-Bet Shean in the fourth to seventh centuries. Dumbart Oaks Pap 51:85–146
Waldmann N, Anselmetti FS, Ariztegui D, Austin JA, Pirouz M, Moy CM, Dunbar R (2011) Holocene mass-wasting events in Lago Fagnano, Tierra del Fuego (54 degrees S): implications for paleoseismicity of the Magallanes-Fagnano transform fault. Basin Res 23:171–190. doi:10.1111/j.1365-2117.2010.00489.x
Wechsler N, Katz O, Dray Y, Gonen I, Marco S (2009) Estimating location and size of historical earthquake by combining archaeology and geology in Um-El-Qanatir, Dead Sea Transform. Nat Hazards 50:27–40. doi:10.1007/s11069-008-9315-6s
Wells DL, Coppersmith KJ (1994) New empirical relationships among magnitude, rupture length, rupture width, rupture area, and surface displacement. Bull Seismol Soc Am 84:974–1002
Wetzler N, Marco S, Heifetz E (2010) Quantitative analysis of seismogenic shear-induced turbulence in lake sediments. Geology 38:303–306. doi:10.1130/G30685.1
Yagoda-Biran G, Hatzor HY, Amit R, Katz O (2010) Constraining regional paleo peak ground acceleration from back analysis of prehistoric landslides: example from Sea of Galilee, Dead Sea transform. Tectonophysics 490:81–89
Yeats RS, Sieh K, Allen CR (1997) The geology of earthquakes. Oxford University Press, Oxford, 576 p
Yechieli Y (1993) The effects of water level changes in closed lakes (Dead Sea) on the surrounding groundwater and country rocks. PhD thesis, Weizmann Institute, Rehovot
Zak I, Freund R (1966) Recent strike-slip movements along the Dead Sea rift. Isr J Earth Sci 15:33–37
Zilberman E, Amit R, Porat N, Enzel Y, Avner U (2005) Surface ruptures induced by the devastating 1068 AD earthquake in the southern Arava valley, Dead Sea Rift, Israel. Tectonophysics 408:79–99